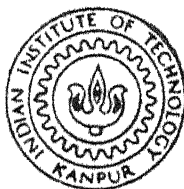


# MATHEMATICAL MODELLING OF PARTICLE SUSPENSION IN PACHUCA TANKS

*By*

**Varshni Singh**

TII  
ME / 1992/M  
Su 641m



DEPARTMENT OF METALLURGICAL ENGINEERING  
**INDIAN INSTITUTE OF TECHNOLOGY KANPUR**

**NOVEMBER 1992**

# MATHEMATICAL MODELLING OF PARTICLE SUSPENSION IN PACHUCA TANKS

*A Thesis Submitted*

in Partial Fulfillment of the Requirements

for the Degree of

Master of Technology

by

Varshni Singh

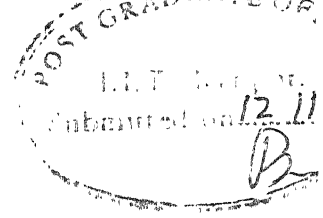
to the

DEPARTMENT OF METALLURGICAL ENGINEERING

INDIAN INSTITUTE OF TECHNOLOGY KANPUR

NOVEMBER 1992

# CERTIFICATE



It is certified that the work contained in this thesis entitled "*Mathematical Modelling of Particle Suspension in Pachuca Tanks*", by "*Varshni Singh*", has been carried out under my supervision and that this work has not been submitted elsewhere for a degree.

---

Dr. Rajiv Shekhar  
Asth. Professor  
Department of Metallurgical Engineering  
Indian Institute of Technology  
Kanpur

November 1992

1993

114836

ME-19912-M-SIN-MAT

# ABSTRACT

The air agitated tanks are used in a number of process industries, including metallurgical industry where these are known as Pachuca tanks. A review of literature shows that no generalized correlation is proposed to obtain the minimum gas flow rate as a function of design and processing parameters to obtain complete off-bottom particle suspension. In the present work a mathematical model is proposed to predict the critical superficial gas velocity (in full-center column) with respect to tank as a function of important design and process parameters like particle diameter, solid concentration, draft tube dimension, etc. The validity of the model proposed in present work is checked by comparing the results predicted by this model with the available experimental results obtained by Koide et al. for bubble columns with draft tube. On comparison it was found that of the two approaches used first approach predicts relatively better results. Also some modifications in approach 1 were done and checked but the results did not improve significantly. Therefore approach 1 is to be used for calculating  $U_{gc}$ .

# ACKNOWLEDGEMENTS

To acknowledge the help and affection of all the people known to me would perhaps be impossible, nor would it be in any way a measure of my gratitude for them. However as a duty it is sacred.

I am highly indebted to my guide for his assiduous guidance and constant encouragement throughout this work. But for his sheer perseverance and kind attentions . this thesis would not have been in the present state.

If it is not possible to enumerate names of all the close friends, it is equally impossible to forget few of them. Among them is Niraj, the maggu, my partner of marathon inning in front of the boob -tube. It will be impossible to forget his help in compiling this thesis. Himanshu, Katto, Sabu, Kabutar, Brutus, Tunnu, Phatta and many more will always haunt my fondest thoughts for having provided many moments of blissful companionship in every walk of life in these years.

VARSHINI SINGH

# Contents

ABSTRACT	iii
ACKNOWLEDGEMENTS	iv
1 INTRODUCTION	1
1.1 Pachuca Tanks . . . . .	2
1.2 Research Objective . . . . .	5
2 Previous Study	6
2.1 Bubble Dynamics . . . . .	8
2.2 Gas Holdup . . . . .	9
2.3 Suspension of Particles . . . . .	10
3 FORMULATION AND APPROACH TO SOLUTION	13
3.1 Approach 1 . . . . .	19
3.2 Approach 2 . . . . .	22
4 RESULTS AND DISCUSSION	26
4.1 Solids Concentration . . . . .	26
4.2 Particle Diameter . . . . .	27
4.3 Draft Tube Length . . . . .	27
4.4 Draft Tube Diameter . . . . .	31

4.5	Reversal Losses Coefficients . . . . .	33
4.6	Friction Factor Correlation . . . . .	34
4.7	Correlating Single Phase Flow To Multiphase Flow . . . . .	39
<b>5</b>	<b>SUMMARY AND COCLUSIONS</b>	<b>49</b>
5.1	Scope of Further Research . . . . .	50
.1	Tables . . . . .	55



# Chapter 1

## INTRODUCTION

Gas agitated reactors are used in a number of process industries, including the metallurgical industry, where they are commonly known as Pachuca or Brown tanks. These are widely used for leaching ores in the hydrometallurgical production of non-ferrous metals like gold, uranium, zinc and copper. Another example of the use of gas agitated reactors in metallurgical industry is argon stirring of molten steel in ladles. However, it is the chemical and biochemical industries where these are used extensively. Here these are called bubble columns or airlift reactors, and used in a wide range of processes such as coal liquifaction, fermentation, hydrogenation of organic compounds, air oxidation of organic and inorganic compounds, waste water treatment, etc.

Principal objectives in the operation of gas agitated reactors are the suspension of particles, mixing of reagents, mass transfer between air bubbles and the slurry. The important design parameters for the Pachuca tanks are flow regime, bubble size distribution and coalescence characteristics, and gas holdup. Therefore extensive studies have been carried out, mostly in laboratory scale bubble columns, to determine the effect of different operating parameters such as superficial air velocity, draft tube dimensions, tank design and physical properties of the liquid/slurry on the process

parameters described above. These studies[37] have provided rough guidelines for the modification of bubble columns to achieve high process efficiency in different applications. However, to date, we still do not have any exact guidelines for the design and scale-up of these tanks on a fundamental basis.

The main objective of gas agitated reactor particle suspension is often very sensitive to the superficial gas velocity. However, a review of literature indicates that very little amount of work has been done on it. No generalised correlation is available to predict superficial gas velocity facilitating particle suspension, as a function of various design parameters, draft tube dimensions, particle density, solid concentration, etc. In fact, the superficial gas velocity for obtaining complete off-bottom particle suspension as a function of design parameters can be predicted. This is done by model/correlation developed in this work.

## 1.1 Pachuca Tanks

A stable circulating liquid flow in gas agitated reactors is induced by the apparent density difference between the aerated liquid (usually in the central zone) in the draft tube and the annular region surrounding it. This circulating liquid flow brings settling solids in bottom region of the tank into the top region of the tank. The Pachuca tank bottom are usually conical in shape and a perforated plate is used as a gas distributor. Conical bottom bubble columns were used by Koide et. al.[27]. The difference between Pachuca tanks, bubble columns and argon stirred ladles lies in size and geometry. Pachuca tank diameter varies from 5 m to 10 m, diameter of argon stirred ladles is usually less than 2 m and that of bubble columns is much less than 2 m, usually of the order of 0.15 m. The height-to-diameter ratios of Pachuca tanks lies between those of argon stirred ladles and bubble columns at values ranging from 1.5 to 4. Both Pachuca tanks and bubble columns are also operated with a draft

tube positioned in the center just above the perforated plate. Bubble columns with draft tube are also known as concentric airlift loop reactors. In Pachuca tanks the draft tube diameter to tank diameter ratio is approximately 0.1, whereas in bubble columns it is usually greater than 0.4 and at times become as high as 0.87. The draft tube serves as an airlift device causing the circulation of slurry in the tank, slurry rises in the draft tube and flows downward in surrounding annular space. On the basis of draft tube Pachuca tanks can be classified into three kinds, fig.1 as discussed below:

1. Full center column type - The draft tube extends from just above the air injection point to just below the liquid surface.
2. Stub column type - In this type draft tube starts just above the air injection point and ends just above the conical portion.
3. Free airlift type - In this type no draft tube is present at all.

The main advantages in using Pachuca tanks compared to mechanically agitated systems normally used for leaching are :

1. Less maintenance is necessary due to the absence of moving parts, thus can be used for the treatment of corrosive liquids and abrasive slurries without the problem of corrosion/erosion.
2. Solids can be handled without any erosion problem.
3. Aeration of the pulp can be readily provided for enhanced dissolution rates in the leaching of gold and uranium.

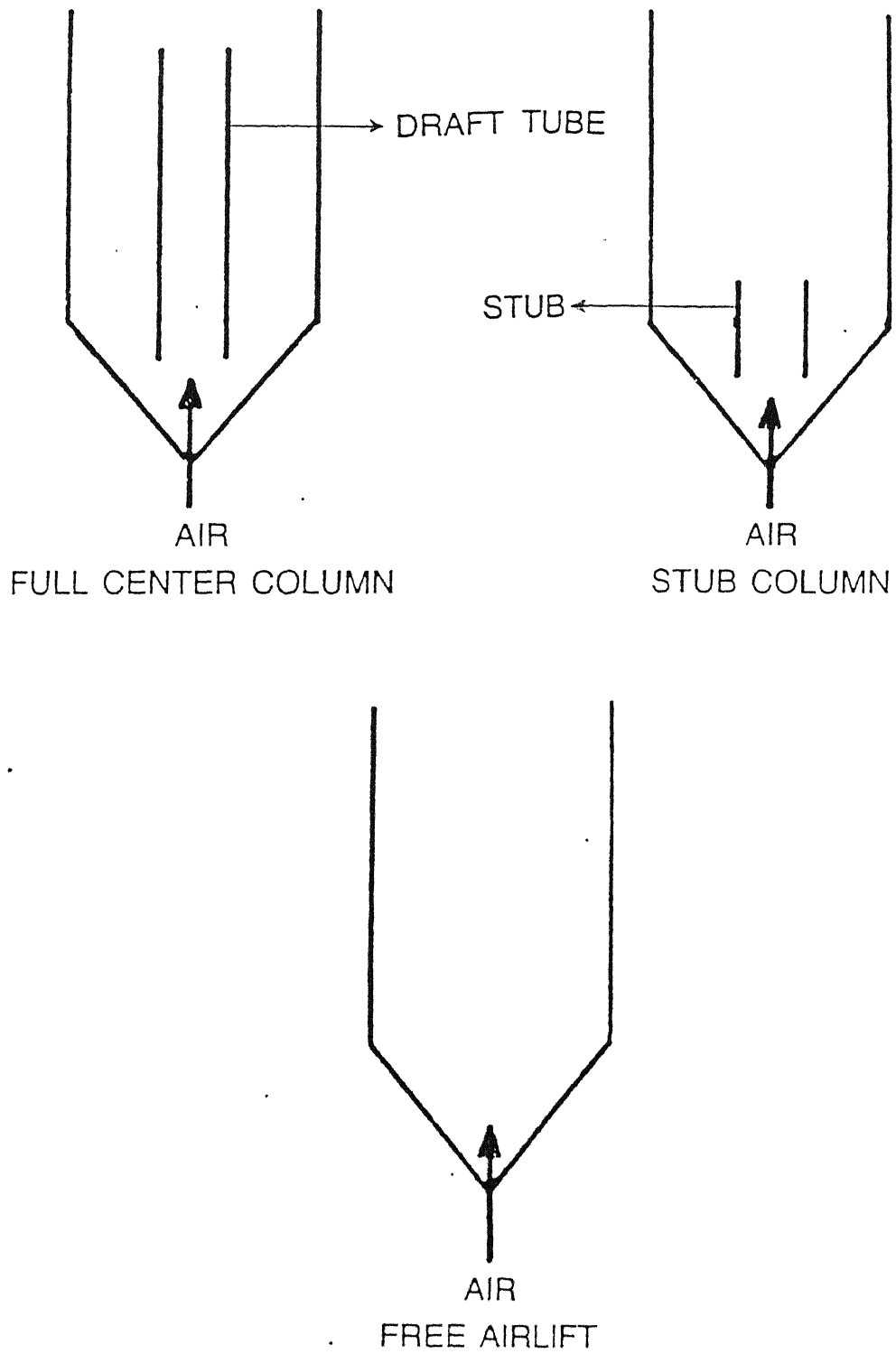


Fig.1 Classification of Pachuca Tanks.

## 1.2 Research Objective

In view of our general ability to define the exact nature of two and three phase flows without direct observation, it is not surprising to find a similar difficulty in predicting pressure drop or energy losses.

The tentative object of the present work is to construct a model for predicting minimum gas flow rate, to obtain complete off-bottom particle suspension in air agitated tanks valid for a relatively large set of data, parameters being particle diameter, particle density, concentration of solids, etc and on this basis to indicate a practical approach for design purposes. Full center column air agitated tanks are considered for the present work. Then the critical gas velocities obtained that from the experimental work of Koide et al.[27] and the model developed in this work are used to explain the effect of various operating and design parameters such as draft tube diameter, draft tube length, particle diameter and concentration of solids.

# Chapter 2

## Previous Study

Shah and coworkers have predicted that in bubble column reactors the hydrodynamics, transport and mixing properties such as pressure drop, holdup of various phases and interphase mass transfer coefficient depend strongly on the prevailing flow regime. Different criteria have been proposed to differentiate flow regimes. Wallis[49] has characterised the upward movement of the bubble swarms into three separate flow regimes. These flow regimes occur in order of increasing gas flow rate.

1. Bubbly Flow or Quiescent Bubbling:

This regime is characterised by bubbles of almost equal size. For this regime the superficial gas velocity should be less than .05 m and the rise velocity of the bubbles in the range .18 to .3 m/s. These data should be regarded as a guideline for two phase (air and water) only.

2. Churn Turbulent Regime or Heterogeneous Regime:

The homogeneous gas-in-liquid dispersion cannot be maintained at higher gas flow rates an unsteady flow pattern with channeling occurs. This heterogeneous flow regime is characterised by large bubbles moving with high rise velocities in

the presence of small bubbles. The large bubbles can grow up to a diameter of about .15 m.

### 3. Slug Flow:

In small diameter bubble columns, large bubbles are stabilised by the column wall leading to the formation of bubble slugs at high gas flow rates.

Hills[17] extended the flow regime maps to high gas and liquid throughputs. The dependence of flow regime on column diameter and gas velocity was estimated. Slug flow occurred in columns of diameter less than .1 m and gas velocity greater than .05 m/s, churn-turbulent flow occurred in columns of diameter greater than .18 m and gas velocity greater than .06 m/s. Homogeneous flow was possible in all dimensions of columns but gas velocity should be low. It is less than .15 m/s for columns of dia greater than .15 m and for less it is less than .05 m/s. The type of sparger, physico-chemical properties of liquid, the liquid velocity can also affect the transition between the flow regimes. Like (i) Slug flow can already occur at very low superficial gas velocity for highly viscous fluids. (ii) Porous spargers with mean pore size less than 150 micro m generally produce bubble flow up to superficial gas velocities of about .05 to .08 m/s. While for perforated plates with orifice diameter larger than 1 mm, bubbly flow is possible only at low superficial gas velocities. For larger orifice diameter bubbly flow may not occur in case of pure liquids. Thus data above for different flow regimes is only approximate. Larger amount of gas can be processed through the reactor in bubbly flow.

In the three phase flow systems, the effect of solid particles on the flow transition has been studied by some investigators (Darton and Harrison, 1975a,b; Jordani et al., 1976; Kara, 1981) Darton and Harrison[9, 10] proposed a trial and error procedure to calculate the value of gas and liquid holdup. Where the liquid holdup is empirically correlated to gas and liquid velocities and the ratio of clear liquid wake volume to

bubble volume.

## 2.1 Bubble Dynamics

Bubble size, bubble rise velocity, bubble size distribution and liquid and bubble velocity have a direct bearing on the performance of bubble columns. Photographic, electrical and optical probe techniques give reliable results only in the homogenous or bubbly flow regime. In case the gas is sparged by single orifices, or perforated or sintered plates, the diameter of generated bubbles is only slightly dependent on the gas velocity. Akita and Yoshida[2] indicates for  $D_c > 0.3m$  bubble diameter becomes independent of column diameter. Koide et al.[26] reported bubble diameters in a 5.5 m diameter column and found larger sizes than those predicted by Akita and Yoshida and Hughmark[18]. This behaviour was attributed to the relatively large orifice diameter and insufficiently developed bubbly flow in axial and radial directions.

Akita and Yoshida[2] found no effect of orifice diameter in bulk region away from sparger. Obviously, a balance between coalescence and breakup rate controlled bubble sizes. Also was reported by Deckwer et al.[11]. But Kumar et al.[28] and Bhavaraju et al.[6] proposed correlations for bubble sizes which involve the orifice Reynolds no. Therefore the effect of the sparger is still not clarified. Bubble diameter depends on the specific gas-liquid system and its properties with respect to coalescence.

Calderbank[8] and Vasalos et al.[40] have reported high rates of bubble coalescence in highly viscous liquids. Bubble breakup is due to differences at the interface caused by external factors. Low viscosity liquid systems are observed to show significant bubble breakup. Usually, small bubbles are desirable as they yield large interfacial areas, which more than offsets decrease in  $k_L$  with decreasing diameter.



## 2.2 Gas Holdup

It can be defined as the percentage by volume of the gas in the two or three phase mix in the column. The gas conjunction with the knowledge of mean bubble diameter, leads to the determination of interfacial area and in turn mass transfer rates between the gas and liquid phase. It depends mainly on the superficial gas velocity, and often is very sensitive to the physical properties of the liquid.

A column diameter greater than 0.15 m is sufficient to obtain the holdup values which are close to the ones obtained in larger diameter column, i.e. scaleup has a very little effect on the gas holdup. Ueyama and Miyauchi[39] analysis yields that the gas holdup in the churn turbulent flow is nearly proportional to  $U_g$  and slightly decreases with an increase in the column diameter.

The extreme sensitivity of the holdup to the material system and to the trace impurities is not well understood due to large scatter in values obtained by Schugerl et al.[36], Bach and Pilhofer[3]. Only a few correlations are based on numerous experimental data of Akita and Yoshida[1]. Hikita et al.[16], Bach and Pilhofer[3], and Mersmann[29].

Jeffery and Acrivos[21] found that for particles as small as a few (  $< 10$  ) microns, suspensions behave macroscopically as non-Newtonian fluids. Therefore, gas holdup values involving the non-Newtonian liquids might be useful in analysing the gas-slurry systems. Hikita et al.[16] concluded that at low gas velocities the single nozzle gas sparger gives lower values gas holdup than a multinozzle or a porous plate sparger.

The presence of solids does not affect the gas holdup significantly. Begovich and Watson[5] combined the available 169 gas holdup points in three phase systems and proposed an empirical correlation. Ying et al.[42] applied correlation by Akita and Yoshida[1] to their data and concluded that the correlation given by Akita and Yoshida is equally adequate for three phase systems.

Kato et al.[24, 25], Ying et al.[42], et al.(1980) concluded that an increase in solids concentration generally decreases the gas holdup, but the effect becomes insignificant at high gas velocities ( $> 0.1m/s$ ).

Freedman and Davidson[13] and Botton et al.[7] empirically observed insignificant effect of the draft tube on the holdup values. On the basis of the other works (Werland,1978) it can be concluded that the effect of the internals on the gas holdup is negligible, and any correlation which fairly represents the values in the presence of internals.

Equations by Akita and Yoshida[1] or Hikieta et al.[16] are recommended for less viscous and coalescing liquids (*viscosity*  $< 0.02 P_aS$ ) . These can also be used for the three phase systems if the solid phase densities are close to water ( $\approx 1000 - 1400 Kg/m^3$ ) .

## 2.3 Suspension of Particles

The adequate degree of suspensuion of solid particles means homogenization of slurry so formed or a near homogenization such that the suspension ensures uniform process conditions leading to predictable results. And the adequate degree of mixing is the required degree of turbulence which minimises the mass transfer resistance.

The suspension is not strictly homogenius although apparently the suspension looks complete. The agitation should be such that the solids are just suspended and the entire solid surface area is exposed to the liquid for any reaction in the vessel. A perfect homogenisation at the further expenditure of energy is not desirable. In fact, it has been establised that further stirring of an already suspended slurry does not increases the mass transfer coefficient appreciably. Thus the suspension criterion is chosen as the condition when no solid particles are resting on the bottom plate of the agitated vessel.

The small pile of particles remain normally for a very short interval at bottom, and at slightly higher speed of liquid, the momentary stay of particles would not exceed a second. At this point Narayanan et al.[31] and Zwietering[44] considered suspension to be complete. At the point of complete suspension, distribution is fairly homogenous when the particles are small and light, whereas coarse and heavy particles remain in the lower part of the vessel(Zwietering, 1958). The homogeneity of the suspension is not influenced noticeably by the shape of the bottom.

Regarding homogeneity of the mixture, Durand and Condolios [12] classified particles. Particles with a diameter of less than  $50 \mu m$  form a homogenous mixture even when the movement of the liquid is very slight. Particles from  $50$  to  $200 \mu m$  do not form a perfectly homogeneous mixture, but when completely suspended particles were distributed over the whole height of liquid, it approaches homogeneity at higher speeds. Particles above  $2 \text{ mm}$  move only by successive jumps along the bottom and remain in the lower part of the liquid. Particles from  $0.2$  to  $2 \text{ mm}$  form a transition category.

In systems with low slip velocity, the turbulence generated by this relative velocity may be negligible in comparison to the turbulent energy being used up to suspend the solid phase and the net effect of the solids is to exert a damping action on the fluctuating velocity of the slurry. But an assumption of no slip velocity between the particle and the fluid introduces an inherent source of error.

The only rule, known for scaling up of an agitator which must keep a solid in suspension is the rule of equal power per unit volume. Zwietering[44] found that the required power per unit volume decreases when increasing the dimensions of the apparatus. The rule of equal power per unit volume is therefore on the safe side. Zwietering summed up the conclusion of this section that a confirmation is found of the validity of the scaling-up rule based on the power per unit volume, with two provisos, one it is conservative because in larger apparatus the power can probably

be lower, and secondly, for radial flow impellers it is more generally valid, in that the ratio of tank diameter to impeller diameter can be varied at the same time.

To effectively transfer matte through a series of stirred tanks, off-bottom suspension of the solids in the liquid phase is essential(P.B.Queneau et al.,1975) An impeller imparts both liquid flow and shear stress to a slurry. Flow lifts the solids off the tank bottom and disperses, injected or induced gas throughout the tank. Shear stress breaks up large gas bubbles and create sufficient turbulence to continually distort the bubbles and to prevent a static interface from forming.

Imafuku et al.[19] observed that the critical gas velocity for complete suspension, mostly depends on the liquid near the gas distributor, while Govindrao[14] pointed out that the particle diameter and bed volume have a strong influence on the axial distribution of solids.

## Chapter 3

# FORMULATION AND APPROACH TO SOLUTION

In the present study we are trying to construct a model for predicting the critical gas flow rate for complete suspension of particles in Pachuca tanks. To obtain this we have used the energy balance approach in Pachuca tanks. At steady state the energy balance equation in the Pachuca tanks is as given below.

$$\dot{E}_g = \dot{E}_a + \dot{E}_d + \dot{E}_{dc} + \dot{E}_{de} \quad (3.1)$$

The terms on the right hand side are energy loss terms and that on left hand side energy input terms.  $\dot{E}_g$  is the sole energy source term inside the tank.  $\dot{E}_a$ , is the energy loss term in annular region, i.e. region between draft tube and walls of tank.  $\dot{E}_d$  is the energy loss in the draft tube.  $\dot{E}_{dc}$  is the energy loss due to sudden contraction and the reversal of slurry in lower part of tank as the slurry enters the draft tube from the annulus.  $\dot{E}_{de}$  is the energy loss due to reversal and sudden expansion of slurry, as the slurry exits from the draft tube and enters annulus.

The energy that is entering the tank through flowing gas, is equivalent to the amount of work done by gas in expanding isothermally (temperature of slurry and

gas is same) inside the tank, and is estimated by using the following equation.

$$\dot{E}_g = \dot{m}_g R T \log \left( \frac{P_2}{P_1} \right) \quad (3.2)$$

Here  $\dot{m}_g$  is mass flow rate of gas,  $R$  is gas constant,  $T$  is the temperature of gas at which it is flowing into the tank, and  $P_1$  is the atmospheric pressure whereas  $P_2$  is that at which gas is entering the tank. The assumptions that are implicit in using the eq[3.2] are that gas is ideal and whole of the energy lost by gas in expanding under isothermal conditions is transferred to the slurry.

Now there are two different types of flow inside the Pachuca tank, namely, three-phase (Gas-Liquid-Solid) flow inside the draft tube and two-phase (Liquid-Solid) flow in the annulus. Therefore the energy losses inside the draft tube and the annulus are calculated separately in the following manner. But in both, draft tube and annular region flow is similar to closed channel flow. All the friction losses terms used are taken from the literature [46]. The following energy dissipation (per unit mass) term is generalised one, for single phase flow in closed channel/pipe.

$$E = \frac{1}{2} (\langle V \rangle)^2 e_v \quad (3.3)$$

Here,  $E$  is the energy dissipated per unit mass,  $\langle V \rangle$  is average velocity of fluid and  $e_v$  is the friction loss factor. Now the friction loss factor is calculated in different conditions in different way as show below.

For sudden contraction,

$$e_v = 0.45 \times (1 - \beta) \quad (3.4)$$

$$\beta = \frac{\text{smaller } x - \text{section area}}{\text{larger } x - \text{section area}} \quad (3.5)$$

for sudden expansion,

$$e_v = \left( \frac{1}{\beta} - 1 \right)^2 \quad (3.6)$$

and for circular tubes/conduits

$$e_v = \frac{L}{R_h} \times f \quad (3.7)$$

$$f = \frac{.0791}{Re^{0.25}} \quad (3.8)$$

$$Re = \frac{\rho \times V \times d_p}{\mu} \quad (3.9)$$

Here,  $f$  is friction factor,  $L$  is the length of tube/conduit and  $R_h$  is mean hydraulic radius.  $Re$  is Reynolds number.  $\rho$  is density of fluid in the pipe,  $\mu$  its viscosity and  $V$  its velocity.  $d$ , is diameter of pipe in which liquid is flowing.

The two phase flow of water and solid in annulus and draft tube is assumed as pseudosingle phase flow. The velocity used in calculating Reynolds number will be of slurry. Viscosity and density used in calculations for Reynolds number are that of slurry calculated in the following manner.

$$\rho_m = \rho (1 - \phi) + \rho_p \times \phi \quad (3.10)$$

$$\mu_m = \mu (1 + 2.5 \phi + 14.1 \phi^2) \quad (3.11)$$

Here,  $\rho_m$  is density of water,  $\rho_p$  is density of solid particles, and  $\mu_m$  is viscosity of water. The details for the overall density of the suspension given by Eq.[3.10] are given in literature[47]. Guth and Simha [15] had given Eq.[3.11] for concentration dependence of viscosity for dilute suspensions of solid spherical particles.

So as to calculate reynolds no. velocity of slurry is required and since velocity of slurry is also not known both slurry velocity and reynolds no. are to be calculated simultaneously, using the iterative loop method. In iterative loop method we assign some arbitrary value to one of the two quantities (in this case velocity of slurry) and the other is calculated (Reynolds no.). Now using the calculated value (of Reynolds no.) we calculate the other quantity (slurry velocity). Here the loop ends and at this point convergence criteria is checked i.e. whether it is satisfied or not. If it is satisfied we come out of the loop otherwise we go back to the loop. Now the value of later quantity (slurry velocity) is used to calculate earlier one (Reynolds no.) and its value is used to calculate earlier one (slurry velocity) and so on till the convergence criteria

is satisfied, which is checked each time we reaches at the end of the loop. Thus both, slurry velocity and Reynolds no. are calculated successively untill and unless the values converge in such a manner that successive values of reynolds no. differ by less than .01

We have used the above energy loss/dissipation terms in our approach after multiplying these by mass flow rate term, to calculate energy dissipated per unit time. The significant energy losses in the annulus are only because of friction between slurry and surrounding walls. These are calculated by the following equation.

$$\dot{E}_a = \frac{1}{2} \dot{m}_a \times (< V_a >)^2 \left( \frac{L}{R_h} \times f \right)_a \quad (3.12)$$

Here,  $\dot{m}_g$  is the mass flow rate of slurry in annular region of tank,  $< V_a >$  is the average velocity of slurry in annulus, L is the height of tank,  $R_h$  is radius of tank, and, f, friction factor is calculated for tank. The energy losses in draft tube due to friction between slurry and walls are calculated using the following equation.

$$\dot{E}_d = \frac{1}{2} \dot{m}_d \times (< V_d >)^2 \left( \frac{L}{R_h} \times f \right)_d \quad (3.13)$$

Here,  $\dot{m}_d$  is the mass flow rate of slurry in draft tube,  $< V_d >$  is the average velocity of slurry in draft tube, L is the length of draft tube,  $R_h$  is the radius of draft tube, and f, friction factor is calculated for draft tube.

At the lower end of the draft tube the slurry enters the draft tube from annular region, this leads to sudden contraction of slurry. The energy dissipated/losses due to sudden contraction is calculated by the equation given below.

$$\dot{E}_{dc} = \frac{1}{2} (< V_c >)^2 \times [ 0.45 ( 1 - \beta ) ] \quad (3.14)$$

The above equation is for the case where liquid is flowing from a larger x-section pipe to smaller x-section pipe, shown in fig.2. This equation does not take into account reversal losses in Pachuca tanks. Here,  $< V_c >$  is the slurry velocity at the lower end



of draft tube, i.e. just inside the draft tube and

$$\beta = \frac{\text{area of } x - \text{section of draft tube}}{\text{area of } x - \text{section of tank}} \quad (3.15)$$

At the upper end of the draft tube the slurry comes out of the draft tube and flows into the annulus, thereby it expands. The energy losses due to sudden expansion is obtained with the help of following equation[].

$$\dot{E}_{de} = \frac{1}{2} \dot{m}_d \times (< V_d >)^2 \left[ \left( \frac{1}{\beta} - 1 \right)^2 \right] \quad (3.16)$$

Here,  $< V_d >$  is average velocity of slurry in draft tube. This equation is for the case where liquid is flowing from a smaller x-section to larger x-section pipe, shown in fig.2. This equation does not take into account reversal losses in Pachuca tanks. But this does not leads to any significant error as is shown later by using the equations that take into account reversal losses too.

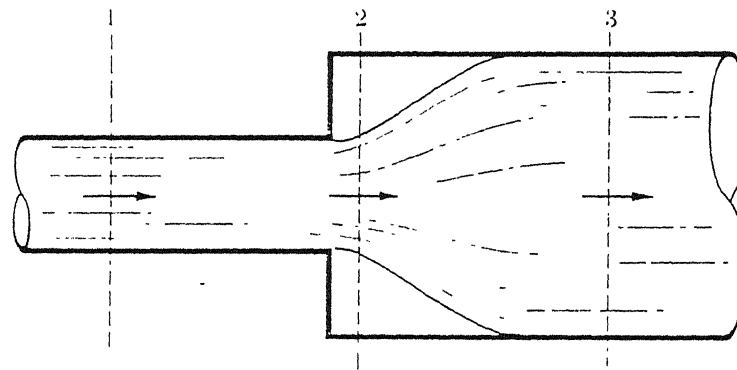
On substituting equations 3.2,3.3,3.4,3.5 and 3.6 in equation 3.1, we get

$$2 A \rho_g R T U_{gc} \log \left( \frac{P_2}{P_1} \right) = \frac{1}{2} \rho_m \left[ \dot{Q}_a \times (< V_c >)^2 \times 0.45(1 - \beta) + \dot{Q}_d \times (< V_d >)^2 \left( \frac{1}{\beta} \right)^2 + \dot{Q}_d (< V_d >)^2 \left( \frac{L}{R_h} f \right)_d + \dot{Q}_a (< V_a >)^2 \left( \frac{L}{R_h} f \right)_a \right] \quad (3.17)$$

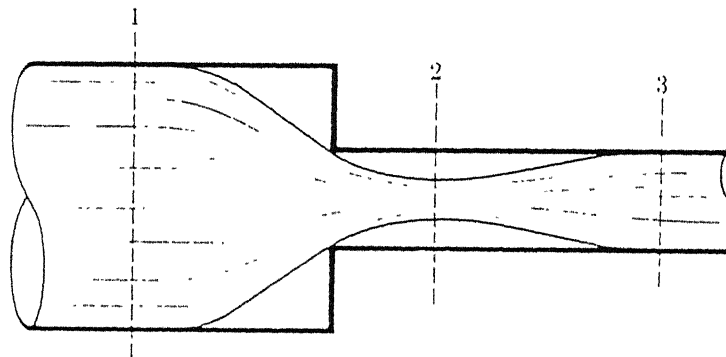
Here,  $\dot{Q}_a$  is volumetric flow rate in annulus and  $\dot{Q}_d$  is volumetric flow rate in draft tube, and  $\rho_m$  is density of slurry. The above equation is rewritten in the following form

$$U_{gc} = \frac{\rho_m}{2 A \rho_g R T \log \left( \frac{P_2}{P_1} \right)} \left[ (V_a)^3 A_a \left( \frac{L}{R_h} \right)_a + (< V_c >)^3 A_d [ 0.45(1 - \beta) ] + (< V_d >)^3 A_d \left( \left( \frac{1}{\beta} - 1 \right)^2 + \left( \frac{L}{R_h} f \right)_d \right) \right] \quad (3.18)$$

In final form of energy balance equation  $< V_c >$ , velocity of slurry near the bottom of draft tube,  $< V_d >$ , the average velocity of slurry in draft tube and  $< V_a >$ , average velocity of slurry in annular region are unknown. To calculate these unknowns two approaches that have been used by us are described in the following lines.



*Sudden expansion.*



*Sudden reduction.*

Fig.2 Sudden Expansion and Contraction in Pipes.

### 3.1 Approach 1

Rose and Duckworth [33] have developed the most systematically based general correlation for the prediction of the pressure gradient. Their correlation is applicable to vertical, inclined, and horizontal pipe flow of gas-solid and liquid-solid suspensions. The correlation developed is based on mechanical energy balance. From their results and the basic elements of their correlation, we have taken the minimum transport velocity for vertical flows.

This equation for two phase flows in vertical pipes is used by us because flow conditions near lower end of draft tube are very much similar to that in two phase flows in vertical pipes. Near the lower end of draft tube flow is nearly two phase flow as bubbles are not dispersed, and their size is quite small. Another reason of using this equation is, Imafuku et al. [19] observed that the critical gas velocity for complete suspension mostly depends on the liquid flow near the gas distributor. Since draft tube and gas distributor, both are centrally positioned in tank draft tube is exactly over the gas distributor. Therefore the slurry flow near lower end of draft tube can be assumed to be same as near the gas distributor.

Therefore,  $V_c$ , the slurry velocity at the lower end of draft tube which corresponds to minimum transport velocity for off-bottom suspension in vertical pipe flows is calculated by following equation

$$V_c = 3.2 \times V_o \times R^{0.1} \times \left( \frac{D_d}{d_p} \right)^{0.6} \times s^{-1.1} \times \left( \frac{V_o^2}{g \times D_d} \right)^{0.25} \quad (3.19)$$

where,  $V_o$  is terminal velocity of particle,  $D_d$  is diameter of draft tube,  $d_p$  is diameter of particle,  $R$  is mass fraction of solids, and  $s$  is ratio of solid density to slurry density. In above equation  $V_o$ , the terminal velocity of particles is unknown. On equating the two equations, one of the gravitational force causing the particle to fall down and the other of drag force resulting from the fall of particle in fluid, we get an equation

which calculates  $V_o$ .

$$V_o = \left[ \frac{4}{3}g \left( \frac{\rho_p}{\rho} - 1 \right) \frac{d_p}{C_D} \right]^{0.5} \quad (3.20)$$

$$C_D = \frac{24}{Re_p} \left[ 1 + 0.1215 \left( Re_p^{0.82} - 0.05 \times \log_{10}(Re_p) \right) \right] \quad (3.21)$$

Equation [3.21] was originally proposed by Beard [5] as a fit to two specific sets of data [4, 32] and agrees closely with all reliable experimental and numerical data in its range, which is 20 to 260 for particles Reynolds number. A portion of the curve of  $C_D$  vs  $Re_p$ , Reynolds number of particles for spheres is reproduced in Fig.3. Table 2 and 3 shows values of Reynolds number and Reynolds number of particles involved in our calculations. Also in these tables are shown corresponding values of  $C_D$ , drag coefficient.

Since now we know  $\langle V_c \rangle$ , we can calculate  $\langle V_a \rangle$ , slurry velocity in annulus by using the mass continuity equation as shown below.

$$\dot{m}_a = \dot{m}_d \quad (3.22)$$

$$\rho_m \times \dot{Q}_a = \rho_m \times \dot{Q}_d \quad (3.23)$$

$$\langle V_a \rangle \times A_a = \langle V_c \rangle \times A_d \quad (3.24)$$

$$\langle V_a \rangle = \langle V_c \rangle \times \frac{A_d}{A_a} \quad (3.25)$$

where,  $\dot{m}_a$  is mass flow rate of slurry in annular region of tank and  $\dot{m}_d$  is that in draft tube.

Inside the draft tube along with slurry gas is also flowing in the form of bubbles. As the bubbles rises their size increases and so does slurry velocity in draft tube. Therefore, to estimate frictional losses in draft tube we calculate  $\langle V_d \rangle$ , average slurry velocity inside the draft tube.  $\langle V_d \rangle$  is calculated by the equation given below.

$$\langle V_d \rangle = \frac{V_c}{1 - \phi_d} \quad (3.26)$$

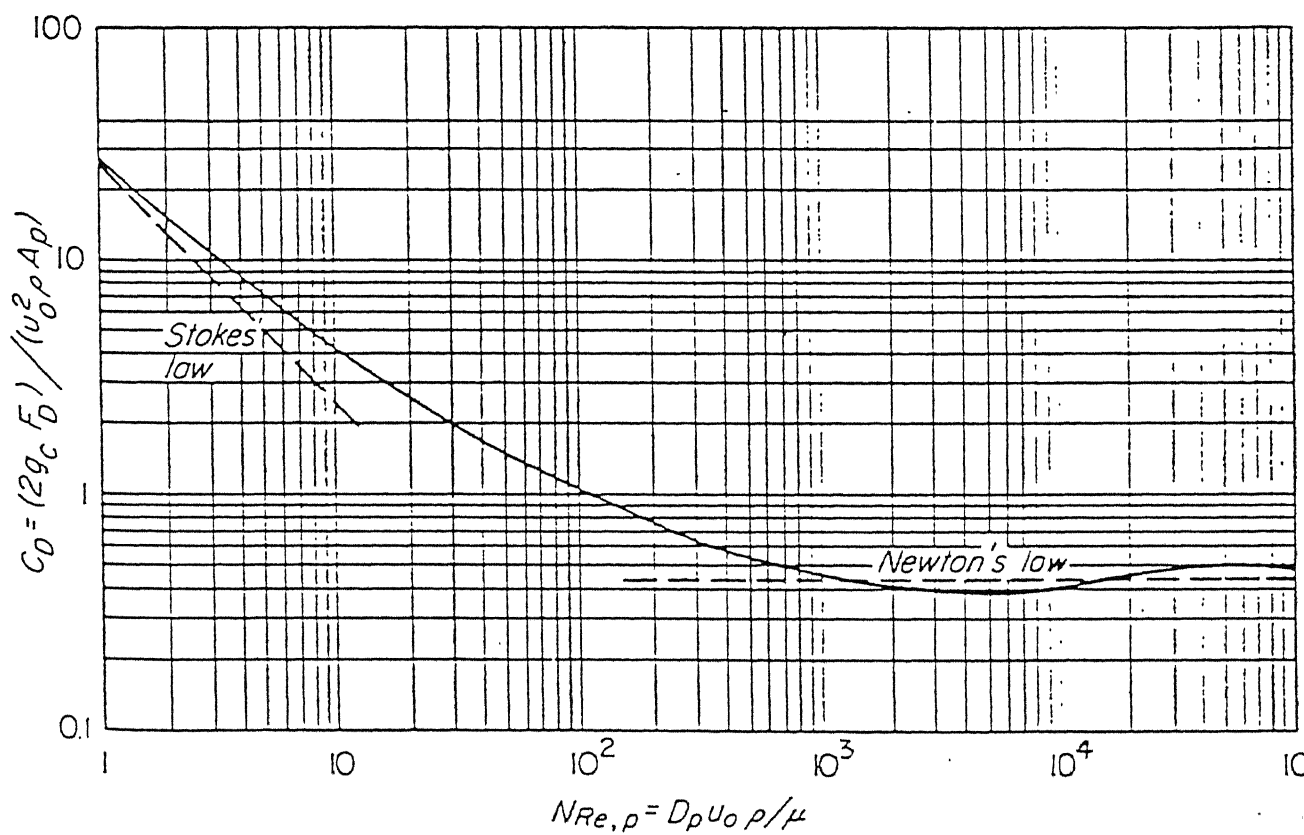


Fig.3 Drag Coefficients for spherical Particles.

$$\text{where, } \phi_d = 1.612 \times U_{gc}^{0.72} d_p^{0.168} D_d^{-0.125} \quad (3.27)$$

$\phi_d$  is the gas holdup in draft tube. In other words, it is defined as volume fraction of draft tube occupied by gas. The presence of solids does not affect the gas holdup significantly. Begovich and Watson [3] combined the available 169 gas holdup points in three phase systems and proposed an empirical correlation

$$\phi_d = (1.612 \pm 0.023) \times U_{gc}^{0.72 \pm 0.028} d_p^{0.168 \pm 0.061} D_d^{-0.125 \pm 0.088} \quad (3.28)$$

$\phi_d$  cannot be calculated directly by eqn[3.26] because  $U_{gc}$  is unknown, therefore eqns[3.26] and [3.18] both will be calculated simultaneously in an iterative loop. The two are calculated successively till the values converge in such a manner that two successive values of superficial gas velocity no more differ than .00001.

## 3.2 Approach 2

It has been observed for baffled tanks, that for small gaps between the turbine and the tank bottom ( $h/H < 1/5$ ) the radial stream pattern dominates [43]. The particles are thrown off towards the periphery, by this radial stream, where they rise along the vertical wall of tank. This is equivalent to saying that the solid phase leaves the near bottom zone at the points where the vertical velocity component of the liquid flowing around the particles reaches its maximum value. The value cannot be less than the terminal settling velocity of particles. Consequently it is reasonable to assume that the minimal flow-around velocity,  $V_p$ , near the bottom that is necessary for off-bottom suspension, should be proportional to,  $V_t$ , terminal settling velocity of particles.

$$V_p \propto V_t \quad (3.29)$$

Suspension of slurry by mechanical mixers usually require a developed turbulent regime ( $Re > 10000$ ) in the tank. Consequently on the tank bottom (or on the

sediment surface) a turbulent boundary layer is created with a velocity profile different from that in the bulk. At the points where the particles leave the sediment, the tangential velocity component of liquid is substantially less than radial one as the measurements indicated [43]. Therefore as a first approximation the stream on this path is considered to be one dimensional. Due to the small thickness of boundary layer the curvature of the sediment is also neglected. Taking these assumptions into consideration Zundeleovich et al.[43] expressed the particle flow-around velocity  $V_p$  near the tank bottom through the relationships defining a one-dimensional flow along the flat plate.

Depending on the particle size,  $d_p$ , and the viscous sublayer thickness,  $\delta_0$ , two possible versions were considered by Zundeleovich, namely

1. If  $d_p < \delta_0$ , the particle is not completely submerged in the viscous sublayer and the average particle flow-around velocity appears to be proportional to the particle ratios.

$$V_p = \frac{0.015 \times d_p \times U_T^2}{Re_x^{\frac{1}{2}} \nu} \quad (3.30)$$

Here,  $U_T$  is the average velocity at the outer border of the turbulent boundary layer.

2. If  $d_p > \delta_0$ , the particle is not completely submerged in the viscous sublayer beyond which the velocity distribution is characterised by the "one seventh" law. The average particle flow -around velocity becomes

$$V_p = U_T \left( \frac{d_p}{x} \right)^{\frac{1}{7}} Re_x^{\frac{1}{35}} - 5 \frac{\nu}{d_p} \quad (3.31)$$

Here,  $x$  is the distance from the flat bottom of the tank. Details are given by Zundeleovich et al.citebib:zu.

Equations [3.29] and [3.30] both includes the unknown value.  $U_T$  the average velocity at the outer border of the turbulent boundary layer, which is close to the

mean bulk velocity in the tank  $\bar{U}$ . The case  $dp > \delta_0$  corresponds to the Newton's sedimentation regime. Within the range of action of Stoke's law and in the almost entire transient range  $dp < \delta_0$ . Though in the Pachuca tanks particle size is of the order of .074 mm but to match the data available we have taken particle size .198 mm. Therefore Eq.[3.30] is used in our calculations. We rewrite the equation[3.30] in the following form

$$U_T = \frac{V_p + 54 \frac{\nu}{d_p}}{\left(\frac{d_p}{x}\right)^{\frac{1}{7}} Re_x^{\frac{1}{35}}} \quad (3.32)$$

Using the same approximation as taken by Zudelevich et al. we replace  $U_T$  by  $\bar{U}$  in equation[3.31] because the average velocity at the outer border of turbulent boundary layer is close to the mean bulk velocity,  $\bar{U}$ , in the tank. Therefore we get

$$\bar{U} = \frac{V_p + 54 \frac{\nu}{d_p}}{\left(\frac{d_p}{x}\right)^{\frac{1}{7}} Re_x^{\frac{1}{35}}} \quad (3.33)$$

We further make an approximation, taking  $V_p$ , flow-around velocity of particles equal to  $V_o$ , terminal settling velocity of particles. We have used the limiting case since  $V_p$ , cannot be less than  $V_o$ . And this  $V_o$  is calculated by equation[3.20], earlier used in first approach. The final equation that we get is as following

$$\bar{U} = \frac{V_o + 54 \frac{\nu}{d_p}}{\left(\frac{d_p}{x}\right)^{\frac{1}{7}} Re_x^{\frac{1}{35}}} \quad (3.34)$$

The above equation calculates minimum, bulk velocity of slurry in the lower part of tank for off-bottom suspension of particles. Now we calculate the velocity of slurry inside the draft tube using the mass continuity equation [3.24], this we rewrite in following manner

$$V_c = U \times \frac{A_a}{A_d} \quad (3.35)$$

This is the slurry velocity just entering the draft tube. To calculate average slurry velocity in draft tube we again simultaneously calculate equations [3.18] and [3.27] in a loop. Initially some value of  $U_{gc}$  is taken arbitrarily and then both are calculated



successively till the values converge to such an extent that successive values of  $U_{gc}$  does not differ by more than 0.00001.

# Chapter 4

## RESULTS AND DISCUSSION

Very limited amount of particle suspension data are available in the literature. The mathematical models described in the previous section are tested with data from Koide et al. [27] work on bubble columns. All the parameters used in our models correspond to those use in his experiments by Koide et el. In order to ensure the validity of the models, results are compared for a large number of parameters such as solid concentration particle diameter, draft tube length and draft tube diameter. In the figures discussed below in this chapter, the solid or broken lines represent the values predicted by mathematical model and symbols represent values obtained experimentally (by Koide et al). The solid particles are of uniform size, with  $d_p = 0.198$  mm and are spherical in shape. The volumetric ratio or volume fraction of solids varied from 0.03 to 0.08 and the size of particles varies in the range 0.117 mm to 0.498 mm.

### 4.1 Solids Concentration

The increase in concentration of solids leads to an increase in slurry density and its viscosity. This in turn leads to decrease in slurry velocity. Therefore to maintain

minimum slurry velocity for complete off-bottom particle suspension higher gas velocity is required. Thus with an increase in concentration of solids the critical gas velocity should increase and our models have predicted the same. Fig. 4 shows that  $U_{gc}$  values predicted by the two models developed matches quite well with those obtained empirically. Therefore both the models predict  $U_{gc}$ , and its dependence on concentration of solids reasonably well.

## 4.2 Particle Diameter

Curve 1 and 2 in fig. 5 represents the two different volume fraction of solids .03 and .08, respectively. Theoretically[46] the slurry velocity should be just the double of terminal velocity of the particles for particle suspension. Empirically it is much higher, but has a direct correspondence with  $V_t$ , terminal velocity. The slurry velocity increases by increasing gas velocity.  $V_t$  is directly dependent on the particle diameter in such a way that as the particle diameter increases  $V_t$  also increases and when particle diameter decreases  $V_t$  also decreases. Therefore, in other words,  $U_{gc}$  increases with increase in particle diameter. Fig.5 shows that approach 1 has predicted  $U_{gc}$  reasonably well though the match is not very good.  $U_{gc}$  increases relatively with a rapid rate with respect to particle diameter/terminal velocity. The same figure as above shows that approach 2 fails to predict  $U_{gc}$  correctly when the parameter is particle diameter/terminal velocity.

## 4.3 Draft Tube Length

In fig.6 there are five distinct sets of data each represented by a different curve. Curve 1, 2, 3, and 4 represent different volume fraction of solid in tank. .03, .04, .06, and .08, respectively. Curve 5 represent that data in which particle diameter is .117 mm,

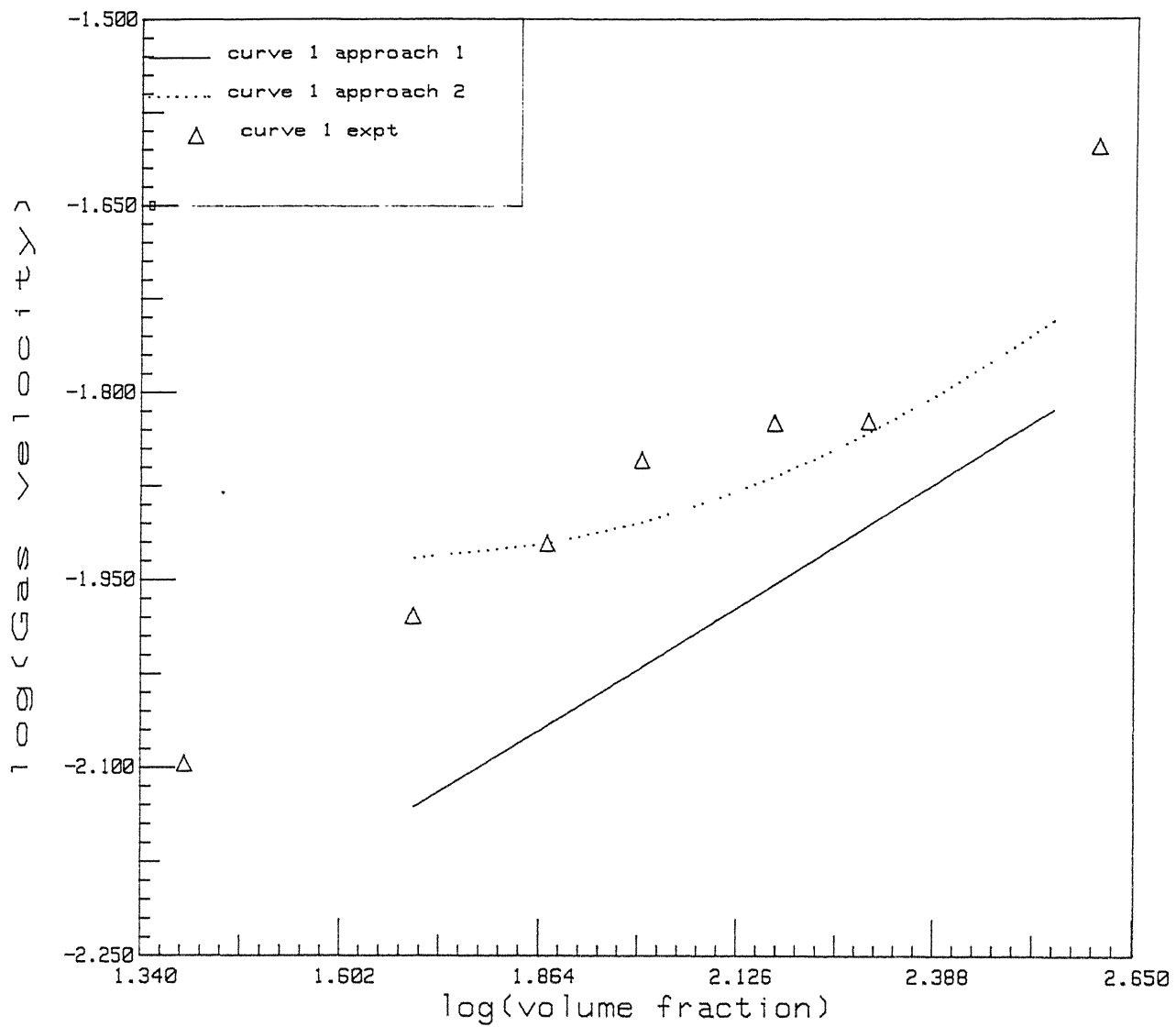


Fig.4 Effect of solid concentration on  $U_{gc}$  and Comparison of  $U_{gc}$  predicted (Lines) by the Two Approaches used and Experimental Data (Symbols) from work of Koide et al.[27].

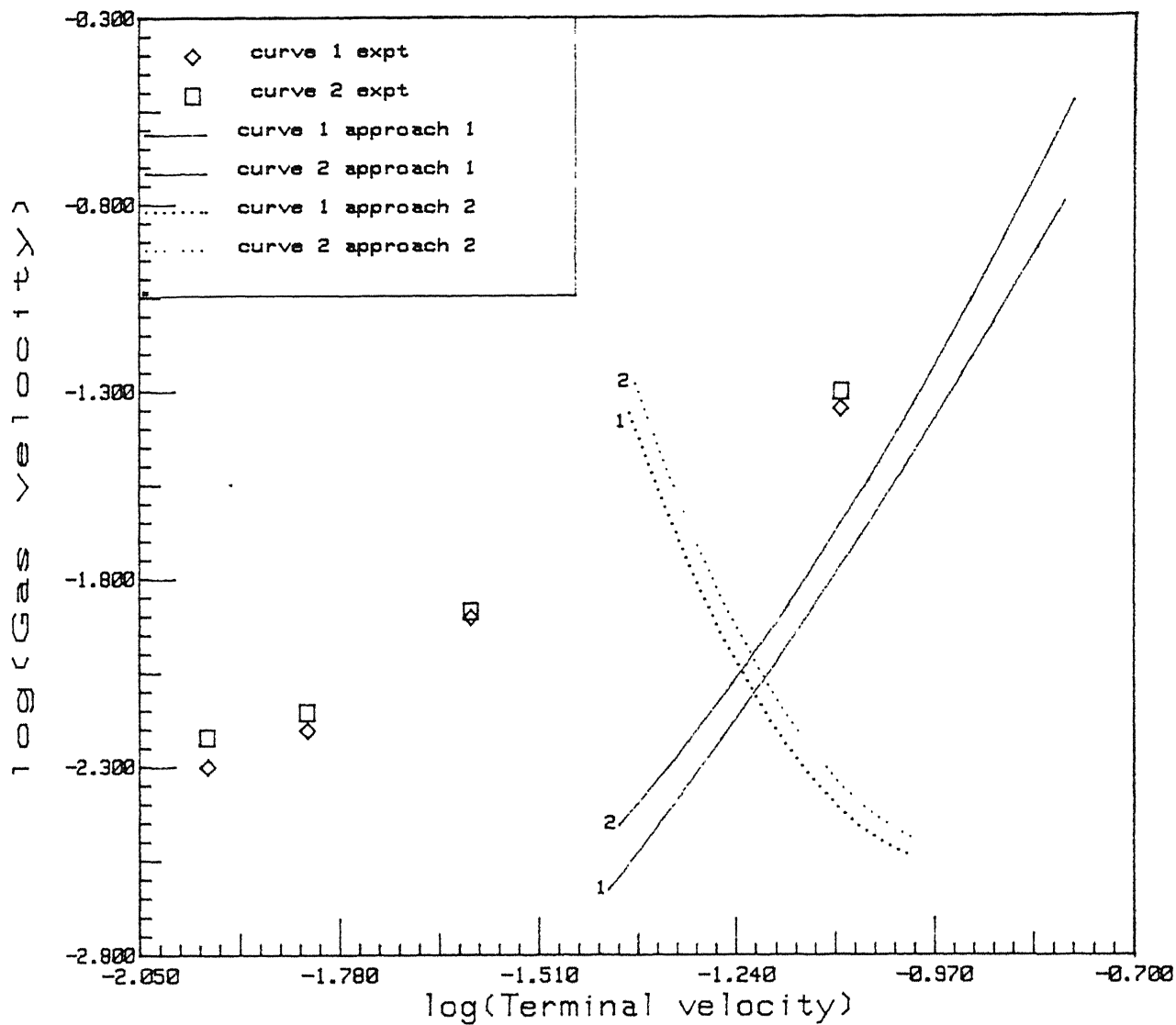


Fig.5 Effect of terminal velocity of particle on  $U_{gc}$  and Comparison of  $U_{gc}$  predicted (Lines) by the Two Approaches used and Experimental Data (Symbols) from work of Koide et al.[27].

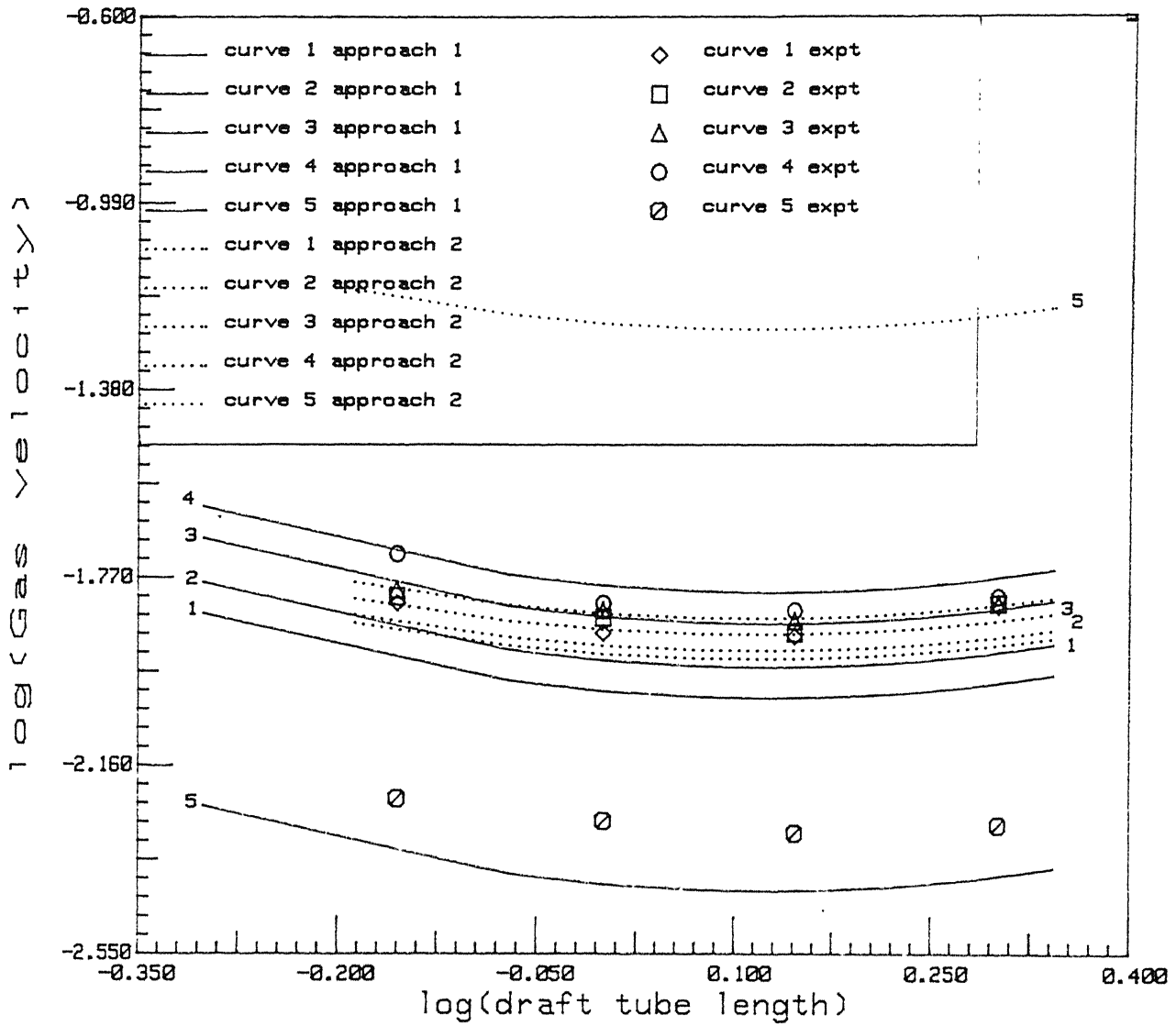


Fig.6 Effect of draft tube length on  $U_{gc}$  and Comparison of  $U_{gc}$  predicted (Lines) by the Two Approaches used and Experimental Data (Symbols) from work of Koide et al.[27].

particle density is  $4680 \text{ Kg/m}^3$  and volume fraction of solids in tank is .04.

Fig. 6 shows that  $U_{gc}$  first of all decreases with increase in draft tube length till the length of draft tube becomes equal to the depth of liquid/slurry, (i.e. when the upper end of draft tube is in level with the slurry at the upper boundary of tank) and after this increases with increase in length of draft tube. The frictional losses in draft tube increases with increase in length of draft tube, and this increase in frictional losses has to be compensated by increase in energy input rate to maintain complete off-bottom particle suspension. Therefore higher gas velocity is required. But the values obtained empirically shows that  $U_{gc}$  decreases with increase in draft tube length, and when draft tube length exceeds the liquid level  $U_{gc}$  increases. Till the draft tube lies within liquid/slurry the slurry velocity inside the annulus increases, therefore the agitation in lower part of tank increases and  $U_{gc}$  decreases. Once it exceeds the slurry level the velocity does not increase anymore but the energy losses inside draft tube keeps on increasing. Therefore  $U_{gc}$  increases to maintain particle suspension. Fig.6 shows that  $U_{gc}$  values obtained empirically are quite close to those predicted by the two approaches. Therefore both the models predict the  $U_{gc}$  values as well as their dependence on draft tube length reasonably well.

## 4.4 Draft Tube Diameter

In fig.7 there are four different curves 1, 2, 3, and 4 for four different values of volume fraction of solid in tank, .03, .04, .06 and .08, respectively. Fig.7 shows that firstly  $U_{gc}$  is decreasing with increase in diameter of draft tube and after a certain value of diameter of draft tube (at which we obtain minimum  $U_{gc}$ )  $U_{gc}$  starts increasing and goes on increasing with increase in diameter.

With increase in diameter of draft tube (keeping the diameter of tank constant), the volume fraction of the tank occupied by the draft tube increases. Since the

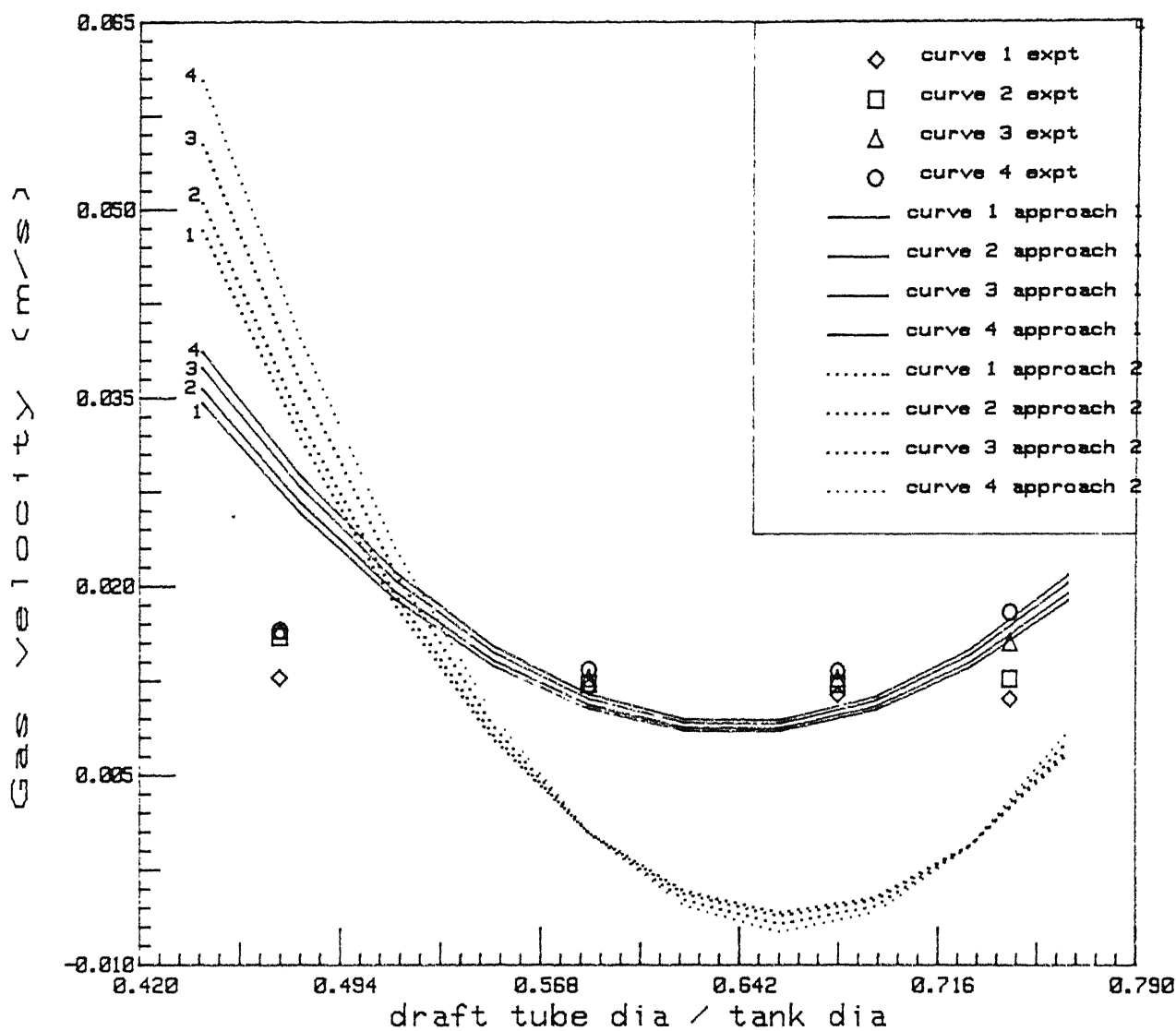


Fig.7 Effect of diameter of draft tube on  $U_{gc}$  and Comparison of  $U_{gc}$  predicted (Lines) by the Two Approaches used and Experimental Data (Symbols) from work of Koide et al.[27].



slurry velocity is expected to be higher within the draft tube compared to annulus, increase in diameter of draft tube leads to decrease in  $U_{gc}$ . Another effect of increase in diameter of draft tube is increase in slurry velocity in annulus. The gas holdup in annular region is mainly determined by the slurry downflow velocity and bubble size distribution. If the effective downflow velocity of the slurry in annulus exceeds the free rise velocities of the bubbles in stagnant liquid, bubbles are sucked into the annular region and swept down by the recirculating liquid. This leads to decrease in hydrostatic driving force ( difference in density of slurry in draft tube and annular region ) for liquid circulation. Firstly the energy losses due to sudden expansion and contraction at the two ends of draft tube decreases with increase in diameter of draft tube. When the area of draft tube diameter equals that of annulus the energy losses due sudden expansion and contraction reduces to zero. Now when diameter is increased beyond this value energy losses at two ends of draft tube due to sudden expansion and contraction comes into play and increases with increase in draft tube diameter.

Fig.7 shows that the values predicted by the model developed using both the approaches, of  $U_{gc}$  matches quite well with those obtained experimentally by Koide et al[27]. The values given by approach 1 shows relatively better match. The minimum  $U_{gc}$  is obtained at the ratio of  $\frac{D_d}{D_t} \approx 0.6$  by Koide et al. experimentally, whereas in the case of model developed it is obtained at the ratio of 0.68 for both the approaches.

## 4.5 Reversal Losses Coefficients

The energy loss coefficient  $e_v$ , for sudden contraction and expansion at the draft tube bottom and top, respectively, is replaced by reversal losses coefficients at the bottom and top of draft tube. i.e.  $K_{rl}$  and  $K_{ru}$ , respectively.

$$K_{rl} = 5.15 \times \left( \frac{A_d}{A_u} \right)^{.5} \quad (4.1)$$

$$K_{ru} = \left[ 1 - \left( \frac{Ad}{Aa} \right)^2 \right] \quad (4.2)$$

The correlation for  $K_{ru}$  has been used quite often and also agrees well with experimental data. However, Koide et al. have suggested that  $K_{ru}$  depends on the height of the liquid level above the draft tube. On the other hand,  $K_{rl}$ , depends on the configuration near the draft tube bottom. If the geometry of the tank is such that it restricts flow from annulus to the draft tube then higher values of  $P_{rl}$  (pressure loss at bottom of draft tube) should be expected. Therefore a tank with a conical bottom (which is the one in consideration), and with a draft tube placed inside the cone should yield higher values of  $P_{rl}$  compared to a tank with flat bottom (that was used by Koide et al. and Miyahara et al.[30]). These were used by Shekhar[38].

The values of  $U_{gc}$  predicted by model using  $K_{ru}$  and  $K_{rl}$  as reversal losses coefficients are comparable to those predicted without using them. How  $U_{gc}$  varies with different parameters and how these values stand against those obtained experimentally are shown in figs. 8 to 11. Fig.12 shows that this model fails in predicting how  $U_{gc}$  varies with draft tube diameter. This is so because  $K_{rl}$  is more sensitive to diameter of draft tube compared to  $K_{ru}$ . Therefore when diameter of draft tube increases  $K_{rl}$  increases much more than  $K_{ru}$  decreases, so energy losses increases. To overcome these energy losses more energy has to be provided. Thus  $U_{gc}$  increases.

## 4.6 Friction Factor Correlation

In approach one we had used much more simple but relatively less perfect correlation for calculating  $f$ , friction friction factor. Here we will use a more perfect and also more complex correlation for  $f$  valid in the full practical range of turbulent flow say,  $3000 < Re < 3,000,000$ .

$$\frac{1}{f} = \left( 4 \times \log( Re \times f^{.5} ) - 0.4 \right)^{-2} \quad (4.3)$$

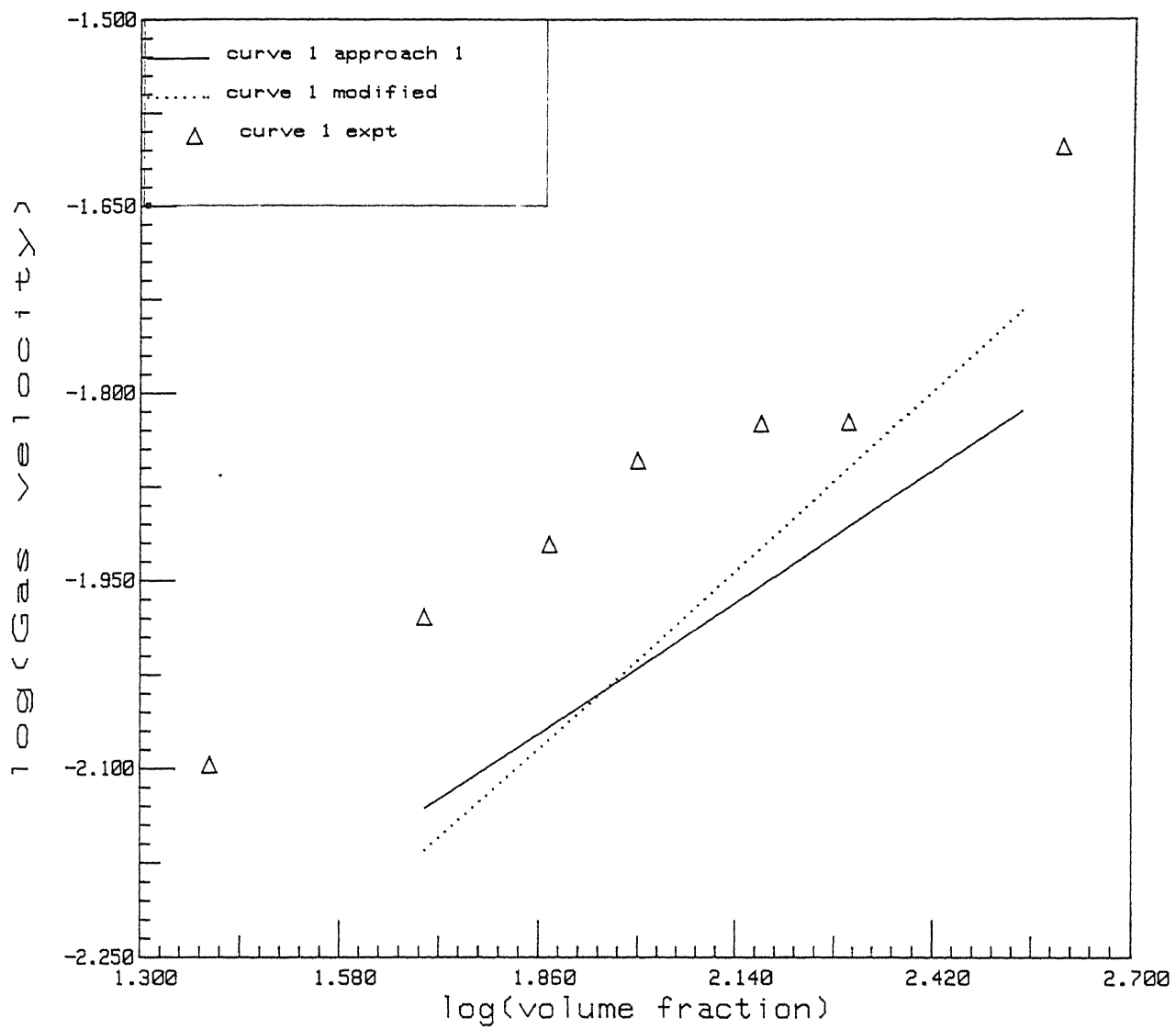


Fig.8 Effect of solid concentration on  $U_{gc}$  and Comparison of  $U_{gc}$  predicted (Lines) by the Two Approaches used and Experimental Data (Symbols) from work of Koide et al.[27].

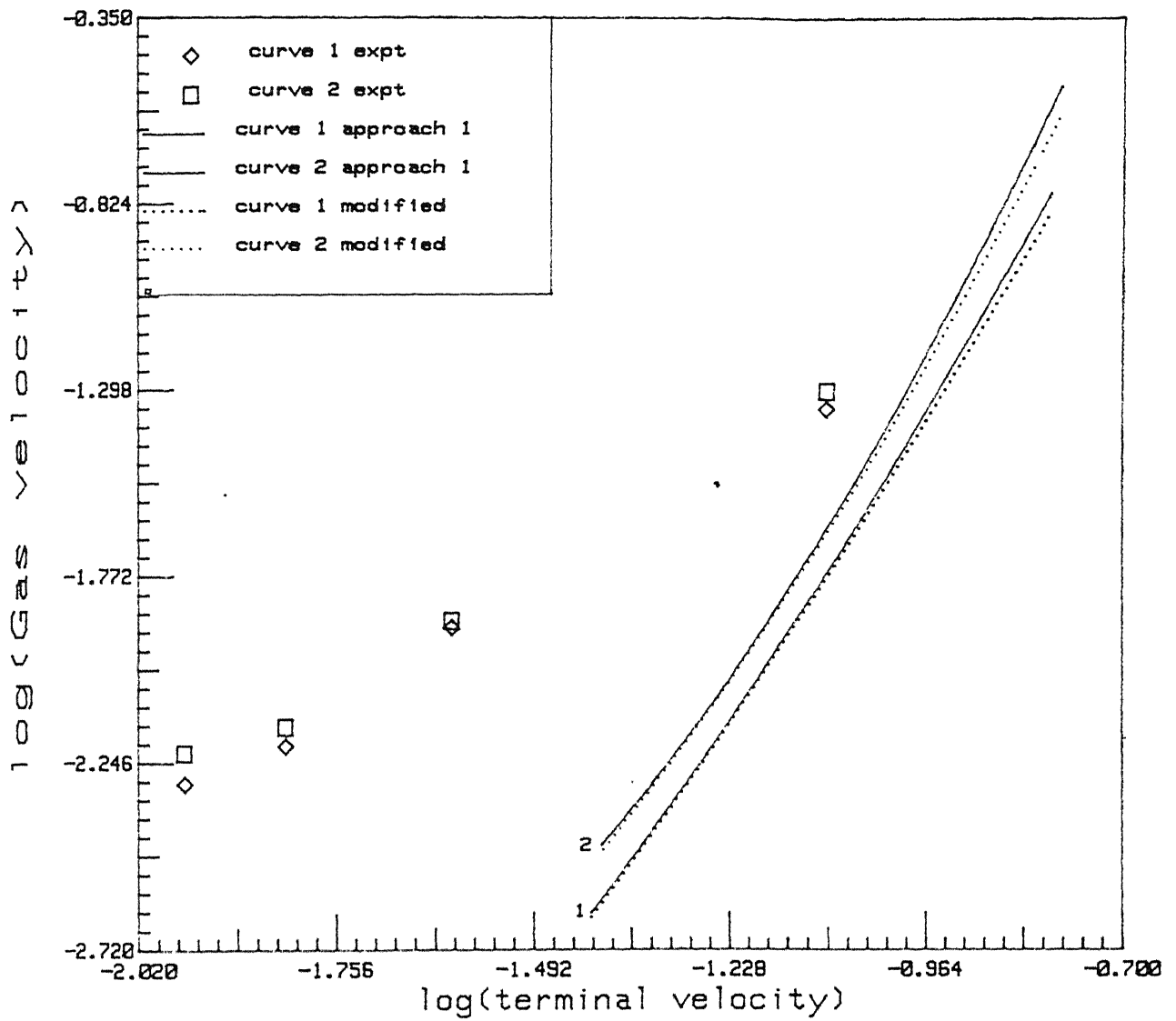


Fig.9 Effect of terminal velocity of particle on  $U_{gc}$  and Comparison of  $U_{gc}$  predicted (Lines) by the Two Approaches used and Experimental Data (Symbols) from work of Koide et al.[27].

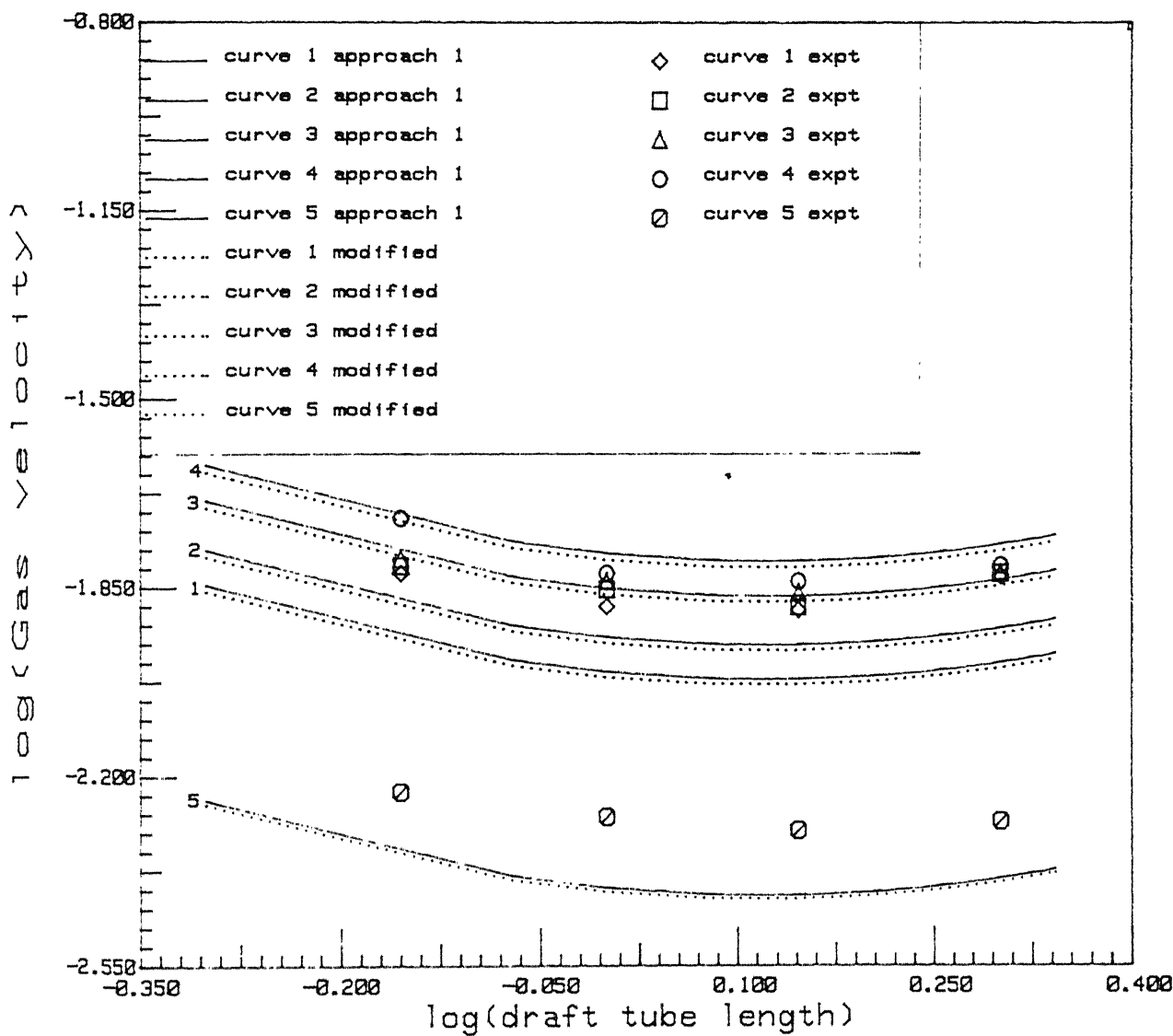


Fig.10 Effect of draft tube length on  $U_{gc}$  and Comparison of  $U_{gc}$  predicted (Lines) by the Two Approaches used and Experimental Data (Symbols) from work of Koide et al.[27].

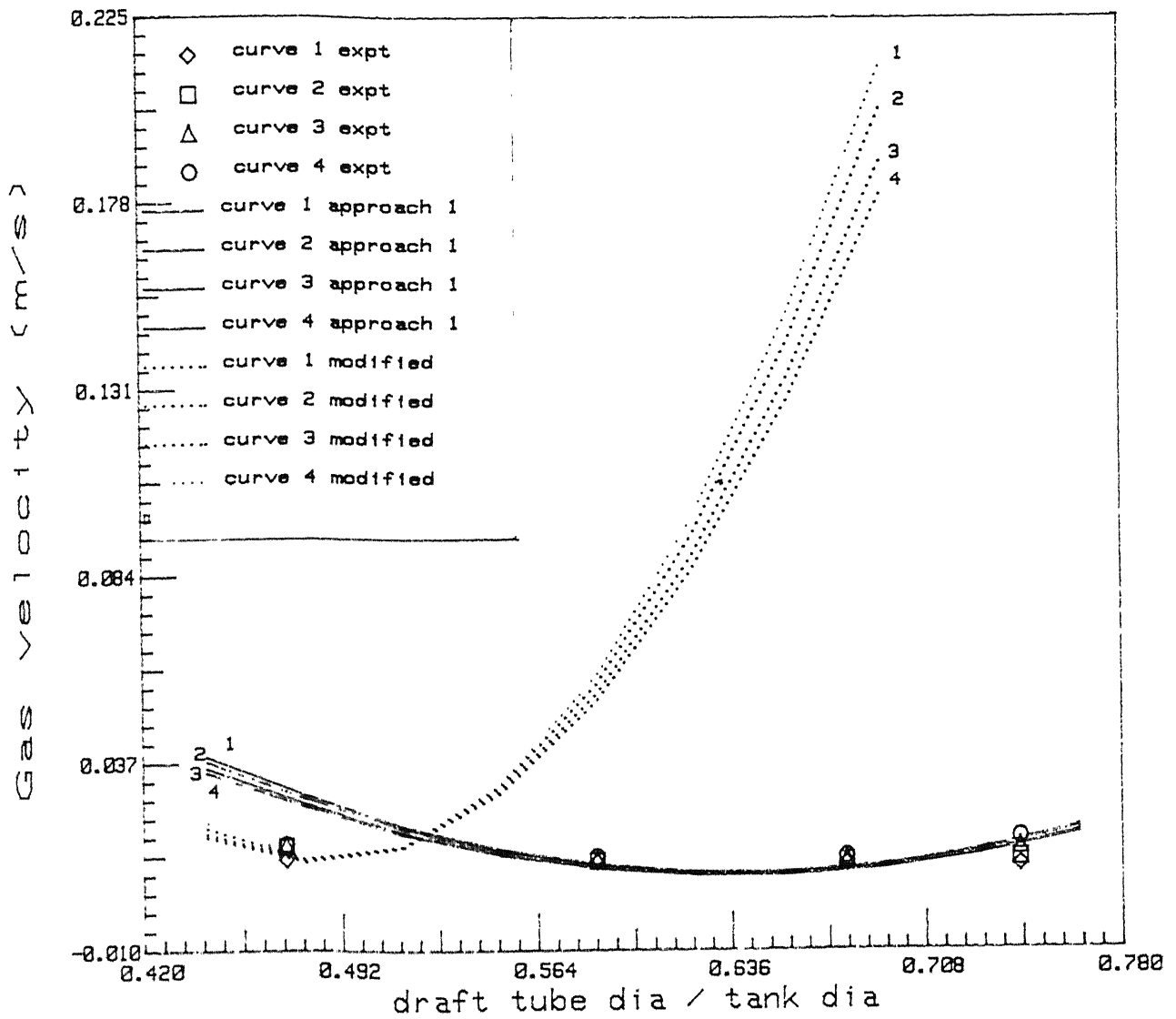


Fig.11 Effect of diameter of draft tube on  $U_{gc}$  and Comparison of  $U_{gc}$  predicted (Lines) by the Two Approaches used and Experimental Data (Symbols) from work of Koide et al.[27].

The above equation due to Nikuradse[46] provides an excellent fit to essentially all reliable data. This equation does not provide us the value of  $f$  directly because  $f$  is also present on right hand side of equation. Therefore it has to be calculated inside a loop till two successive values of  $f$  do not differ by a constant sufficiently small. Eq.[4.3] is based on a form suggested by von Karman(1930) with the constants determined from Nikuradse's data[46]. Figs.12 to 15 shows  $U_{gc}$  values and how it behaves with various parameters. The  $U_{gc}$  values are nearly the same for both cases, i.e. using Eq.[4.3] and Eq.[3.8] for calculating friction factor. But Eq.[4.3] requires lot more calculations to calculate  $f$ , compared to Eq.[3.8]

## 4.7 Correlating Single Phase Flow To Multiphase Flow

In our model we have taken pseudosingle phase flow. Results have shown that it was a reasonably good assumption. Koide et al.[27] have correlated the head losses in three phase flow with the head losses in single phase flow by the following equation.

$$h_3 = \xi \times h_1 \quad (4.4)$$

$$\xi = f^{-1.51} \quad (4.5)$$

Here,  $h_3$  is the head loss in three phase flow,  $h_1$  is head loss in single phase flow whereas,  $f^{-1.51}$  is volume fraction of liquid.

In our model now we use density and viscosity of water instead of slurry. And we multiply  $f$ , the friction factor for single phase by  $\xi$  to obtain friction factor for three phase flow. Using this we calculate all the values of critical superficial gas velocity for off bottom suspension of particles in Pachuca tanks. The results are shown in figs. 16 to 19. We see that hardly there is any significant difference in the values of  $U_{gc}$  obtained using Koide et al. relation and the one we have assumed.

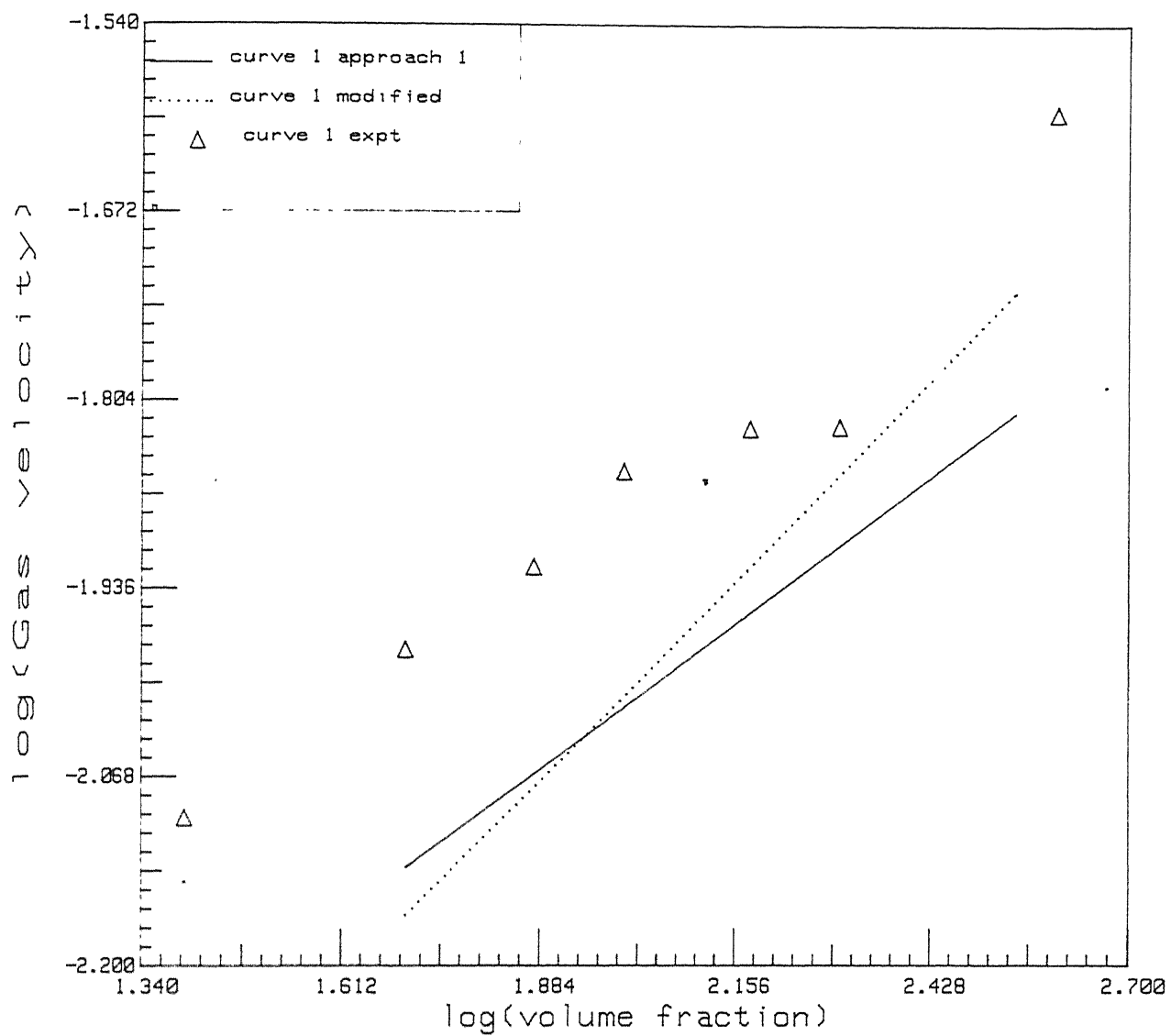


Fig.12 Effect of solid concentration on  $U_{gc}$  and Comparison of  $U_{gc}$  predicted (Lines) by the Two Approaches used and Experimental Data (Symbols) from work of Koide et al.[27].



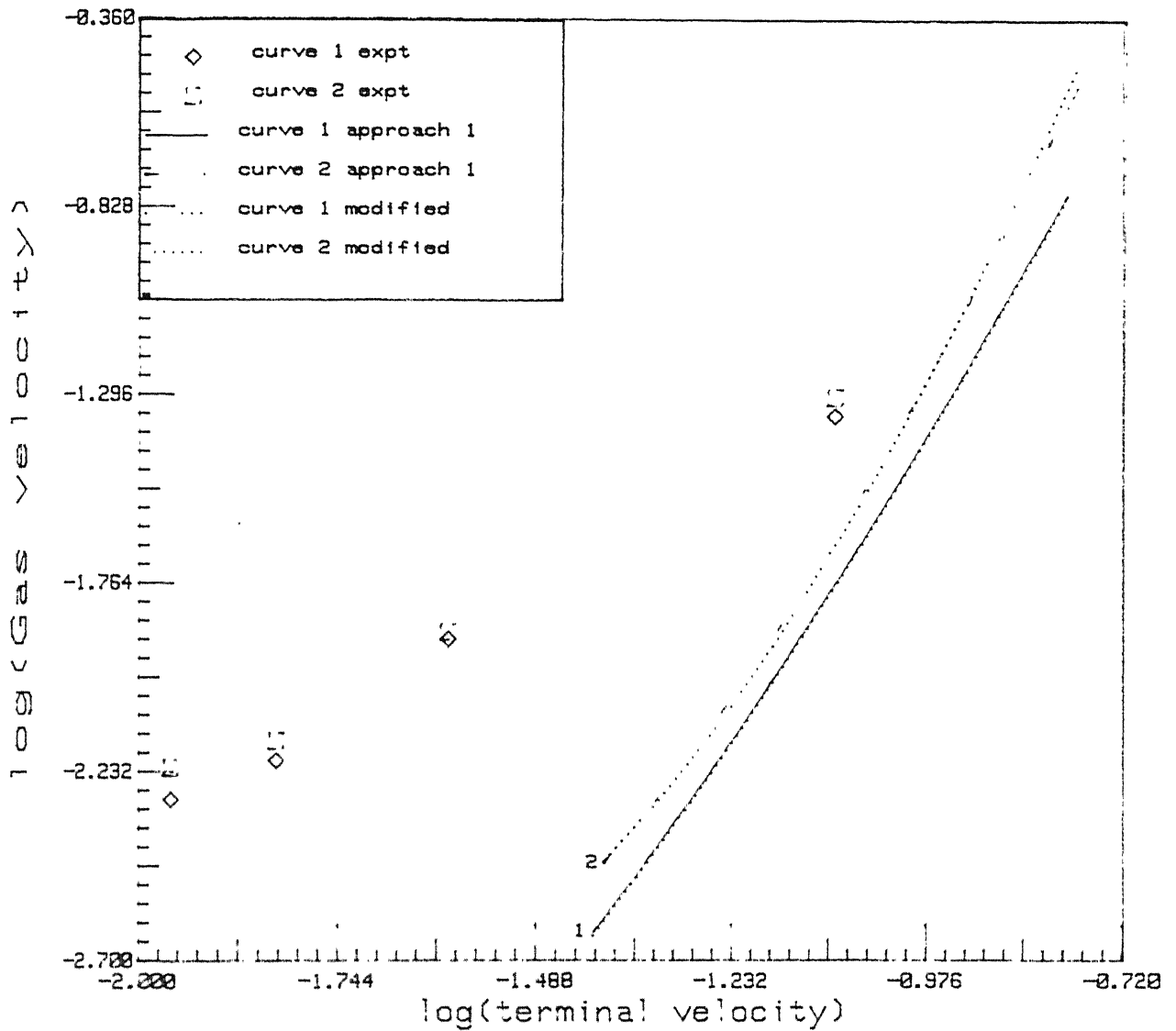


Fig.13 Effect of terminal velocity of particle on  $U_{gc}$  and Comparison of  $U_{gc}$  predicted (Lines) by the Two Approaches used and Experimental Data (Symbols) from work of Koide et al.[27].

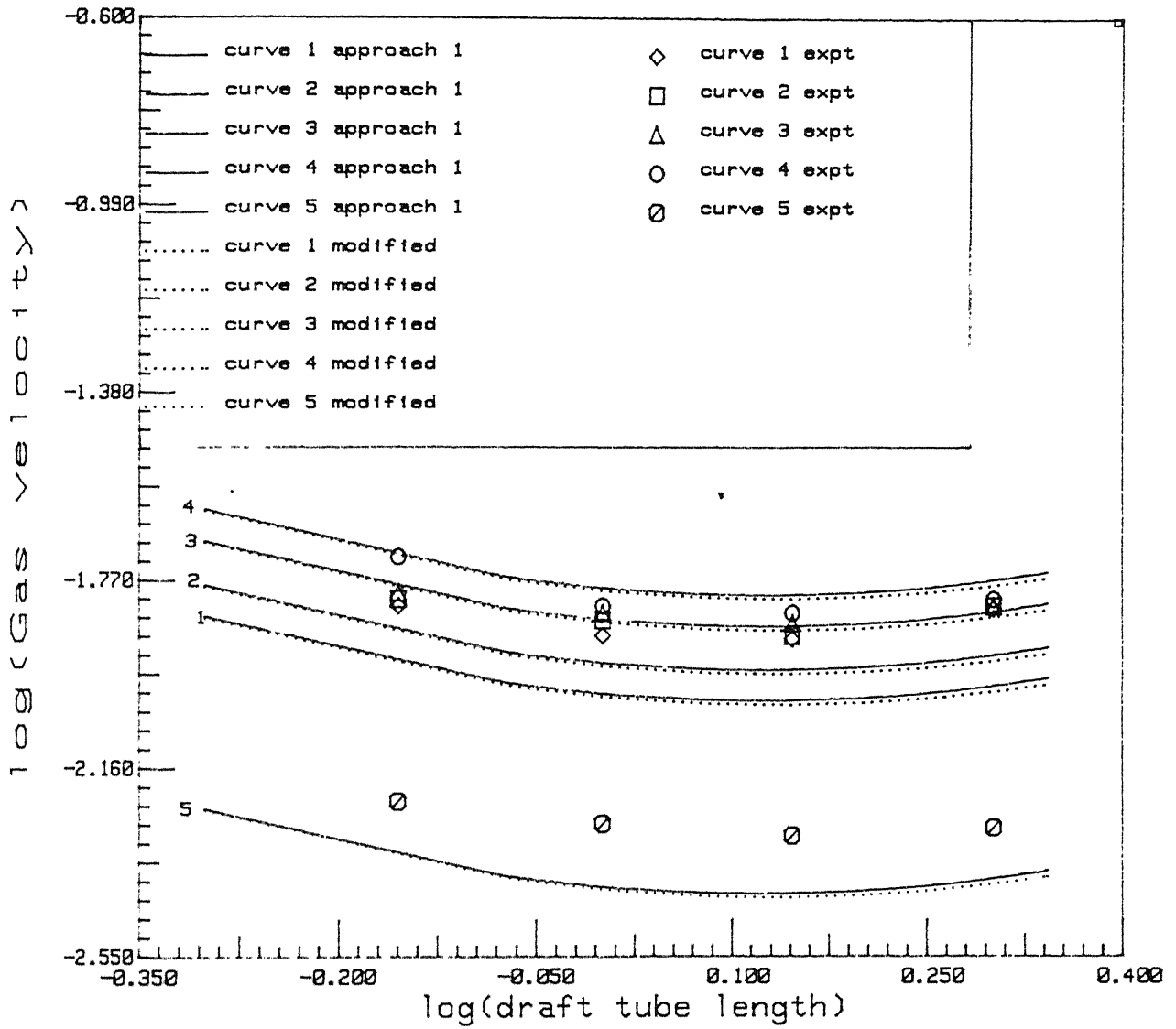


Fig.14 Effect of draft tube length on  $U_{gc}$  and Comparison of  $U_{gc}$  predicted (Lines) by the Two Approaches used and Experimental Data (Symbols) from work of Koide et al.[27].

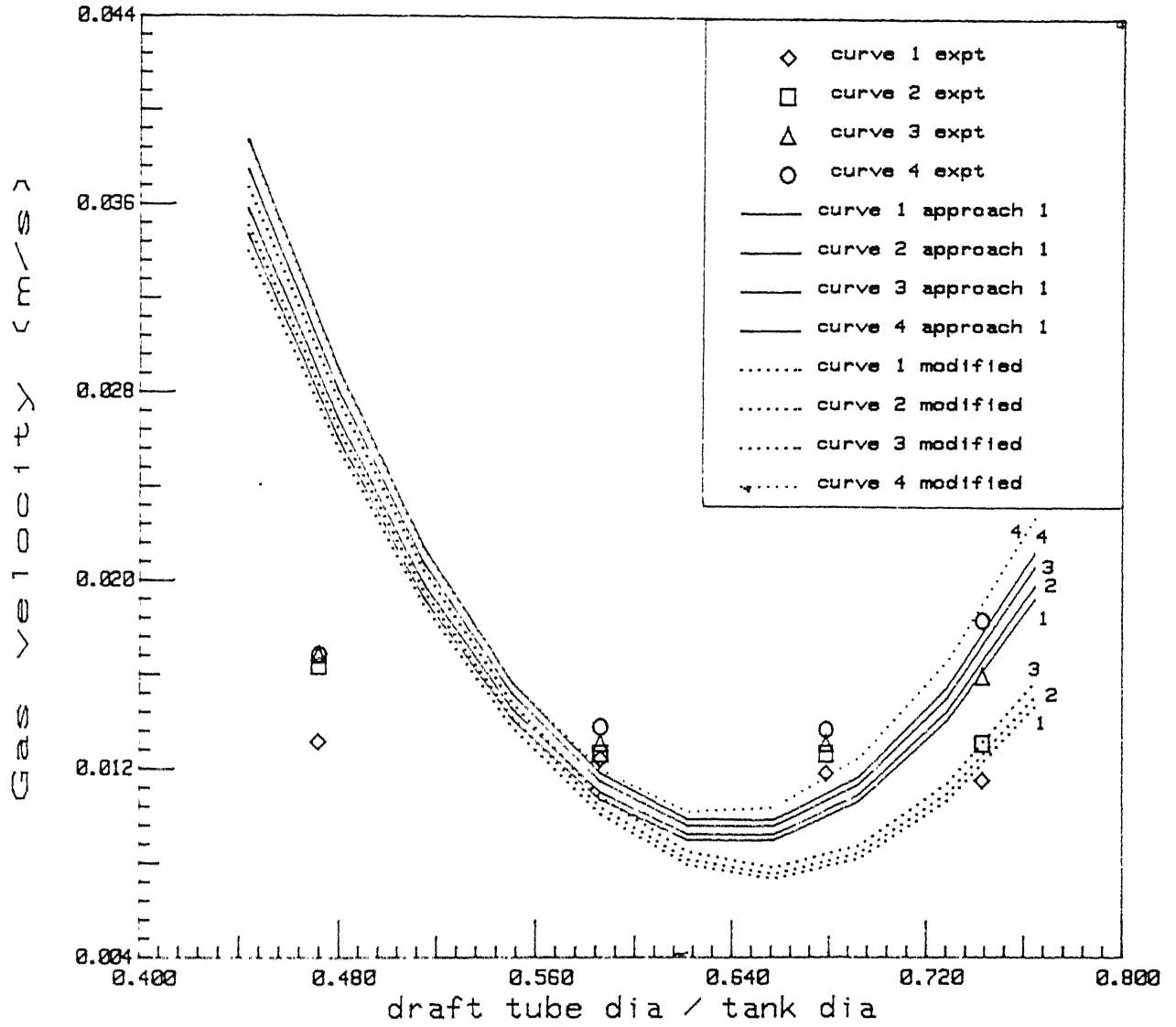
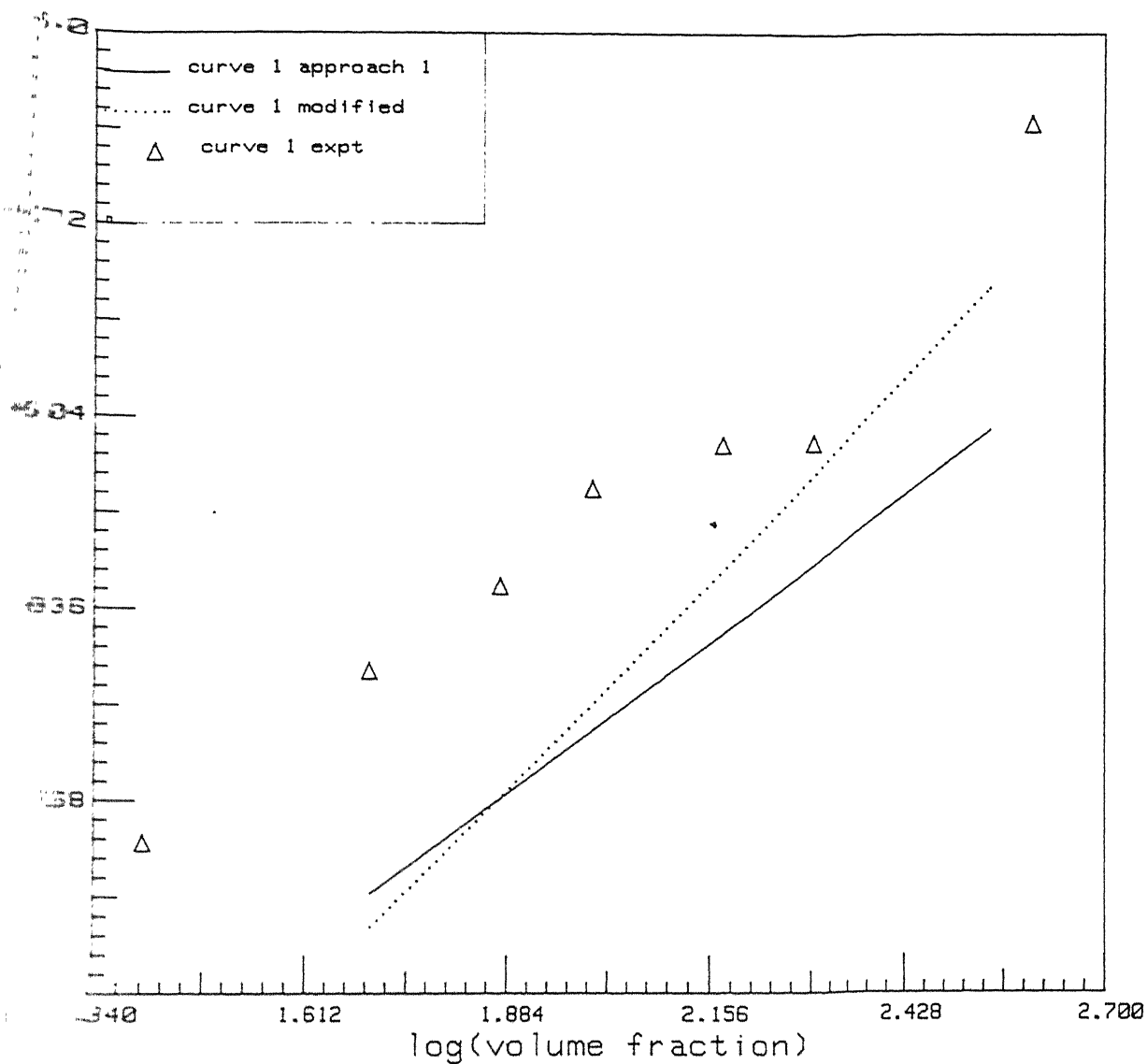


Fig.15 Effect of diameter of draft tube on  $U_{gc}$  and Comparison of  $U_{gc}$  predicted (Lines) by the Two Approaches used and Experimental Data (Symbols) from work of Koide et al.[27].



Effect of solid concentration on  $U_{gc}$  and Comparison of  $U_{gc}$  predicted  
 (es) by the Two Approaches used and Experimental Data  
 (hols) from work of Koide et al.[27].

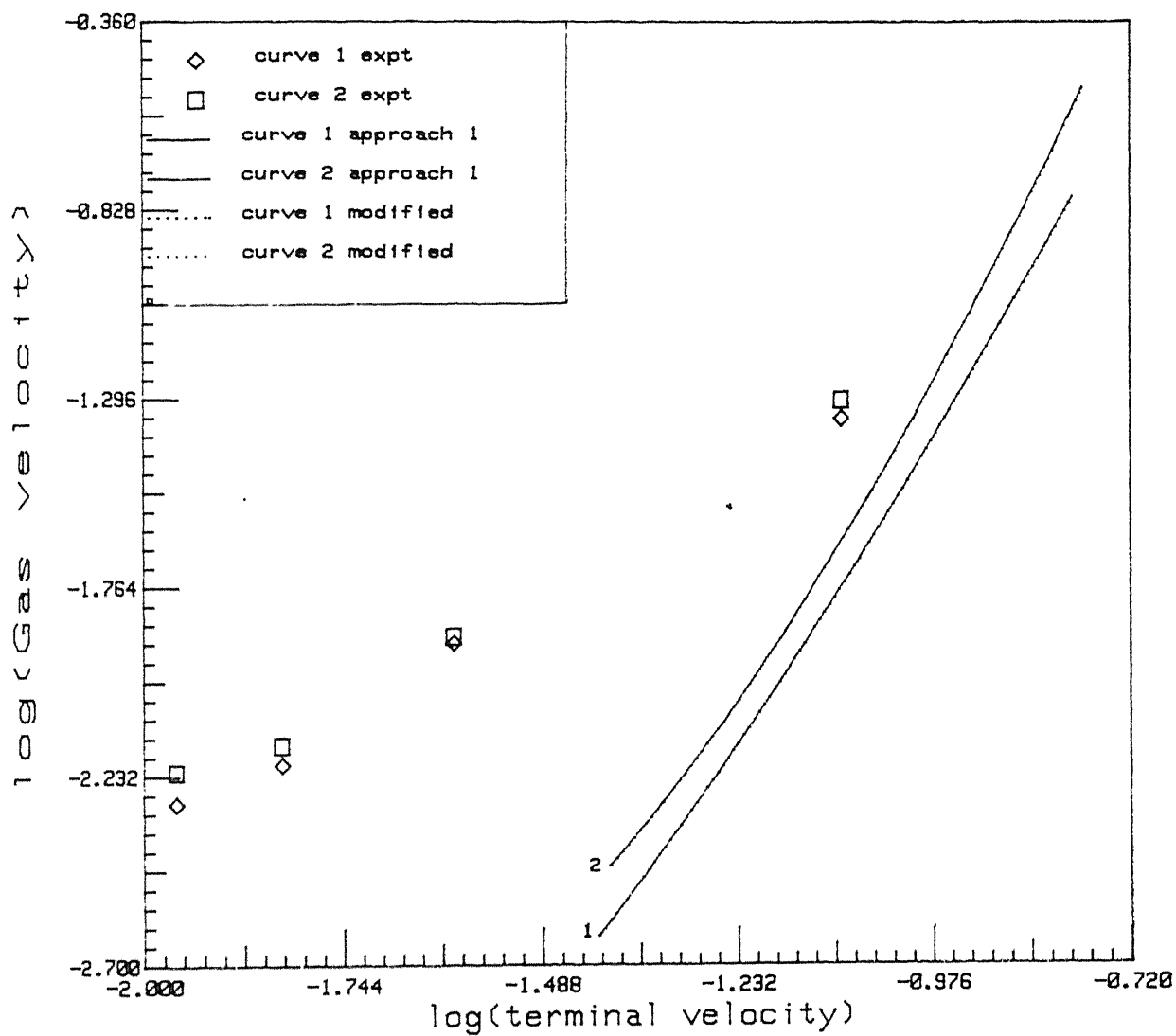


Fig.17 Effect of terminal velocity of particle on  $U_{gc}$  and Comparison of  $U_{gc}$  predicted (Lines) by the Two Approaches used and Experimental Data (Symbols) from work of Koide et al.[27].

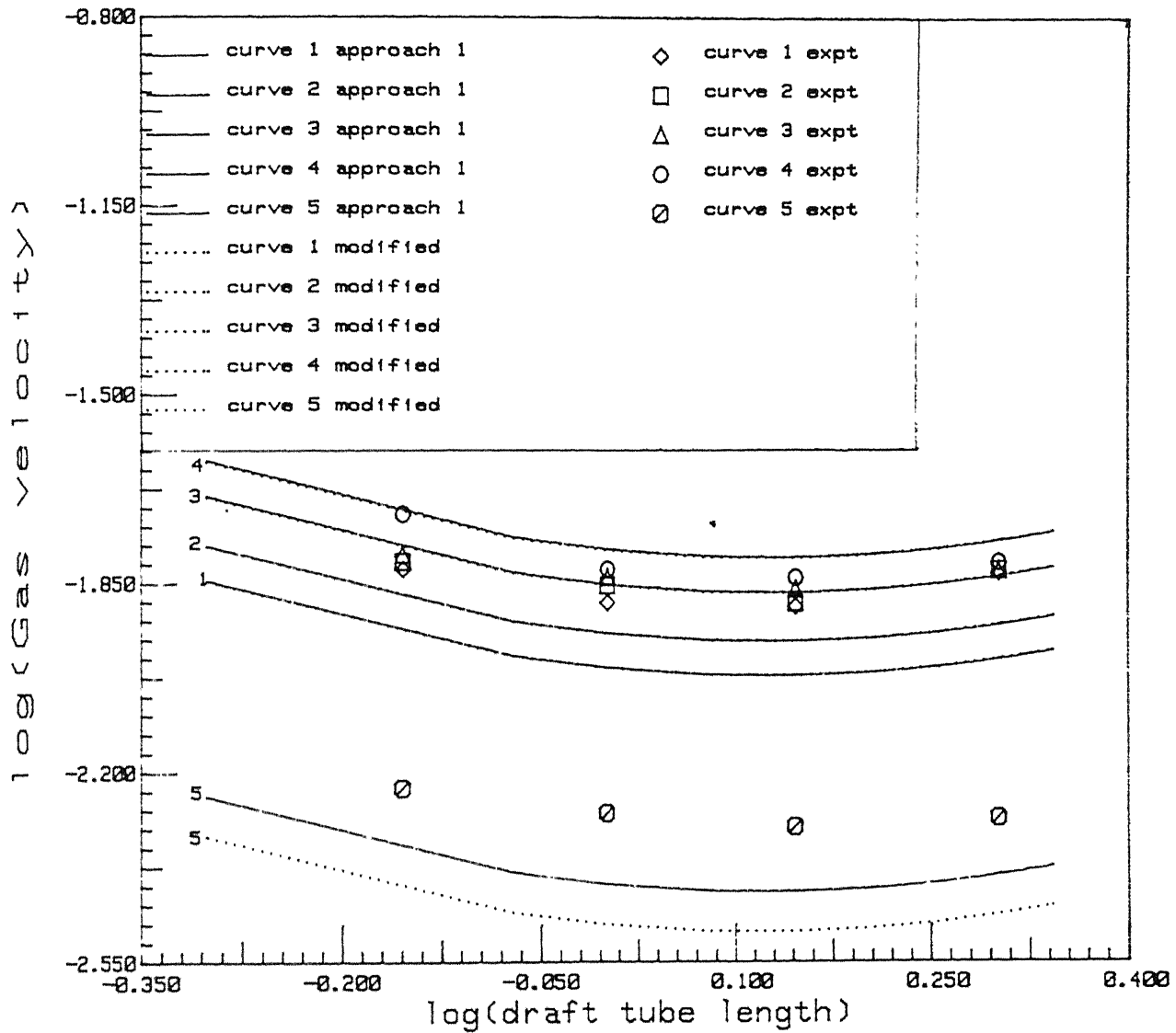


Fig.18 Effect of draft tube length on  $U_{gc}$  and Comparison of  $U_{gc}$  predicted (Lines) by the Two Approaches used and Experimental Data (Symbols) from work of Koide et al.[27].

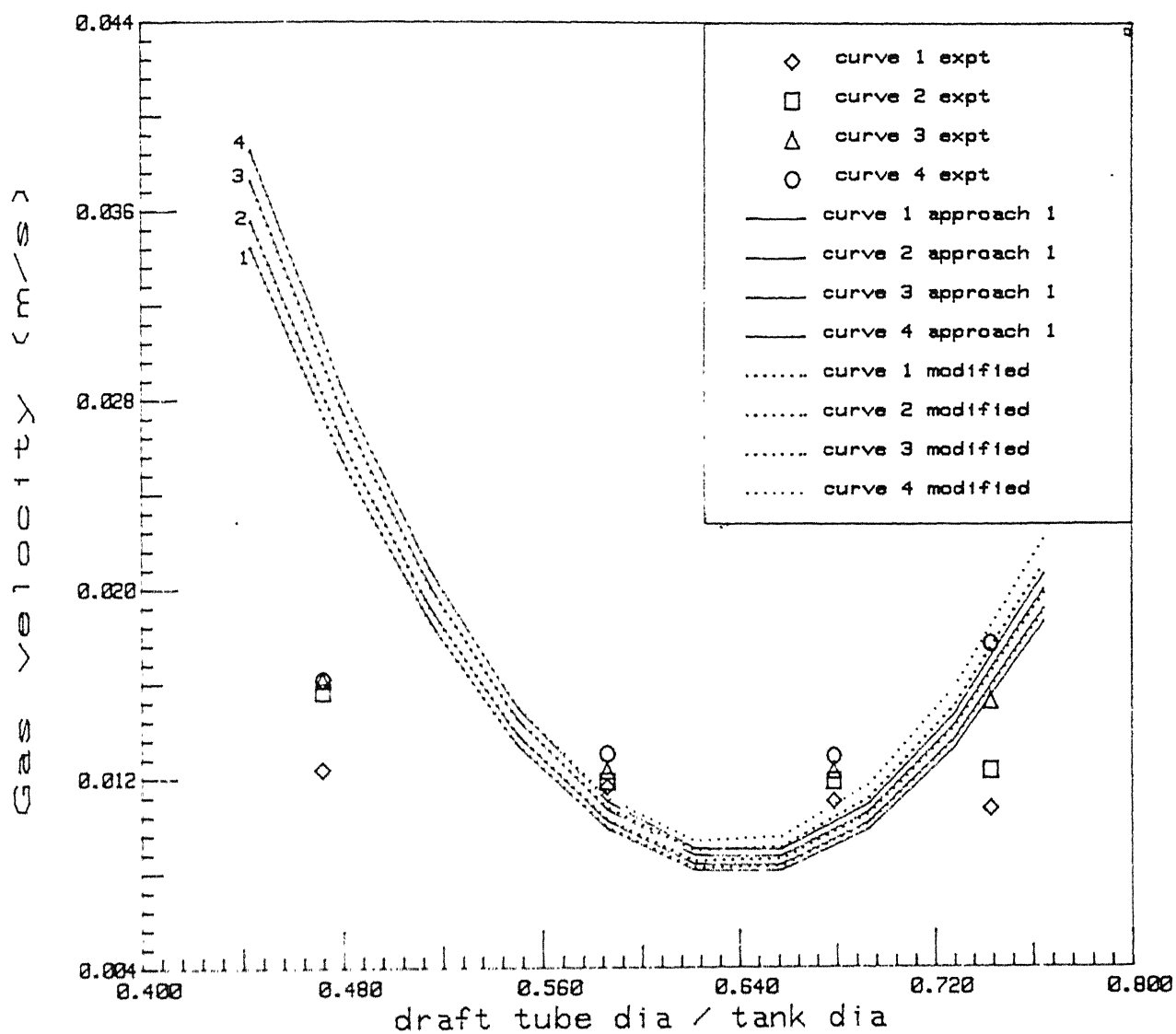


Fig.19 Effect of diameter of draft tube on  $U_{gc}$  and Comparison of  $U_{gc}$  predicted (Lines) by the Two Approaches used and Experimental Data (Symbols) from work of Koide et al.[27].

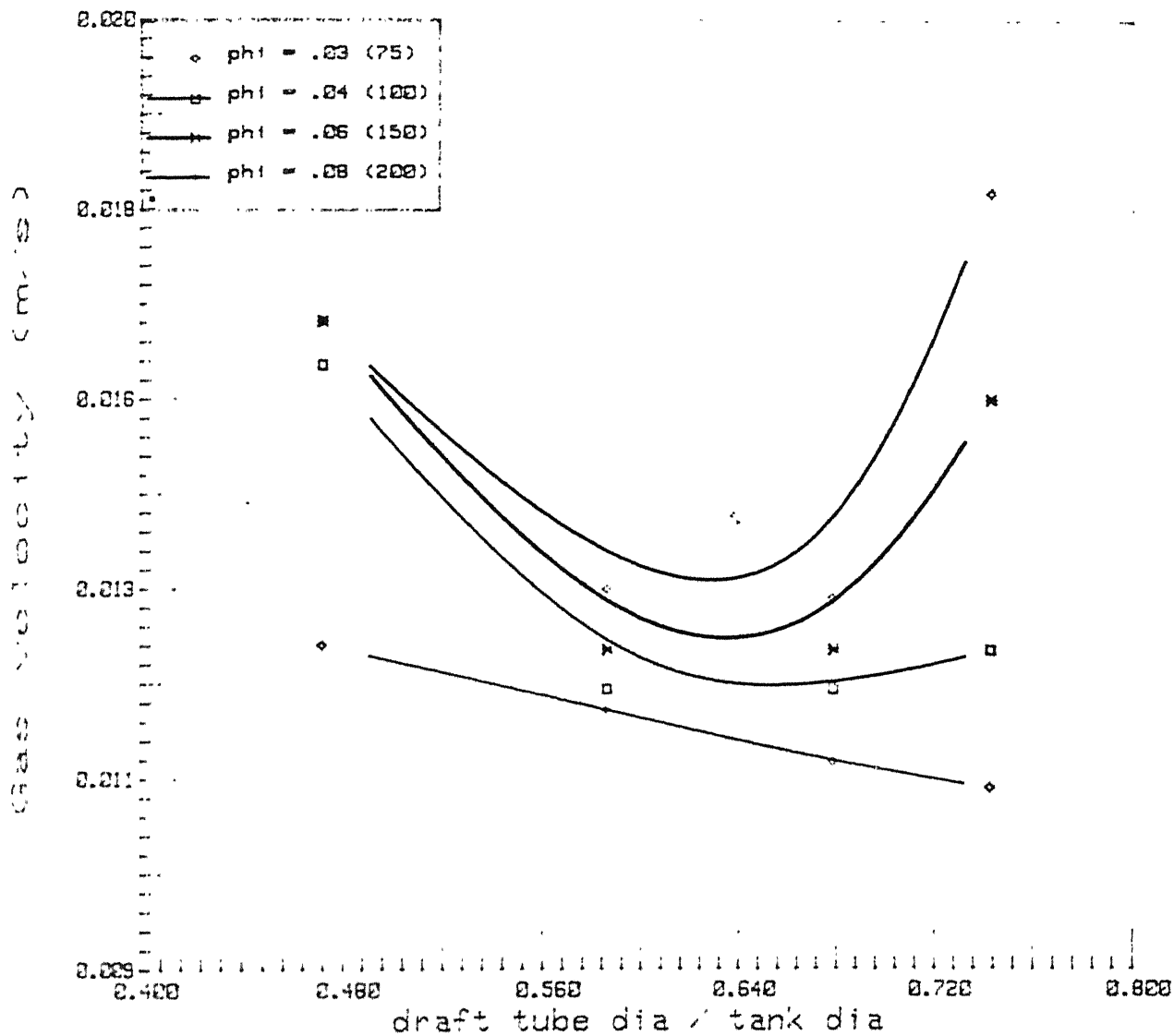


Fig.20 Experimental Values of  $U_{gc}$  Obtained by Koide et al.[27].



## Chapter 5

# SUMMARY AND COCLUSIONS

Gas agitated tanks have been used in the process industry for a very long time. From the engineering point of view the prediction of superficial gas velocity, so as to obtain particle suspension in Pachuca tanks, as a function of various design parameters is quite important. Still very little has been done to propose generalised correlations predicting the superficial gas velocity. Therefore this study proposes a generalised correlation predicting superficial gas velocity and studies the effect of various operating and design parameters such as particle size, solids concentration, and draft tube dimensions on superficial gas velocity for off-bottom particle suspension. These values of  $U_{gc}$  predicted by the proposed model/correlation are compared with those obtained experimentally by Koide et al[27].

This study has proposed a generalised and fundamental correlation that helps us in understanding the dependence of superficial gas velocity, facilitating particle suspension, on important design parameters of air agitated tanks.

1. Increase in concentration of solid particles should lead to decrease in slurry velocity near tank bottom. Therefore particles start settling on the tank bottom. However, on increasing the superficial gas velocity complete off-bottom suspension will be restored.

2. For a fixed tank diameter, increase in draft tube diameter should lead to increase in slurry velocity both in draft tube and annulus. Therefore  $U_{gc}$  decreases, minimum  $U_{gc}$  for off-bottom suspension is obtained at  $\frac{D_d}{D_t} = 0.6$ . Therefore, it seems to be somewhat surprising that industrial scale Pachuca tanks are operated with  $\frac{D_d}{D_t}$  ratios around 0.1.
3. Increase in diameter of particles should lead to increase in terminal settling velocity of particle. Therefore slurry velocity near tank bottom is no more sufficient to keep particles suspended. The slurry velocity is increased by increasing superficial gas velocity to a level when off-bottom suspension is attained
4. Keeping other tank dimensions constant, increase in draft tube length leads to an increase in slurry velocity. Therefore  $U_{gc}$  decreases, minimum  $U_{gc}$  is obtained for certain length of draft tube.

In view of our general inability to define the exact nature of two and three phase flows without direct observation, we also find a similar difficulty in predicting pressure drop accurately. From this point of view the results of our models are quite good. Therefore the models can be used to predict the  $U_{gc}$  to obtain complete off-bottom suspension in air agitated tanks.

## 5.1 Scope of Further Research

Although the correlation proposed is used to predict successfully the empirical gas velocity ( So as to obtain off-bottom particle suspension ) and its dependence on various process and design parameters, the present work prediction could be compared with the available limited experimental data for bubble columns. Therefore it remains to be thoroughly checked for Pachuca tanks. Further to establish its completely generalised form it is essential to compare, the predicted  $U_{gc}$  values for large variation

on the design and operating parameters used in Pachuka tanks, with the experimental data. Because of the difficulties in modelling three phase flows, it is necessary to check the reliability of model by conducting experiments on different aspects of particle suspension. This exercise will also shed some light on the dependence of these process parameters on variables that have not been very well understood.

Therefore the task of determining the superficial gas velocity experimentally for complete off-bottom suspension as a function of various parameters of Pachuka tank and checking the proposed correlation by comparing the values predicted by it with those obtained experimentally is recommended for the future work.

LIBRARY  
114836

## NOMENCLATURE

$A$	cross-sectional area ( $m^2$ )
$A_a$	cross-sectional area of annular region ( $m^2$ )
$A_d$	cross-sectional area of draft tube ( $m^2$ )
$C_D$	drag coefficient
$D$	diameter (m)
$D_a$	diameter of tank (m)
$D_d$	diameter of draft tube (m)
$d_p$	diameter of particles (m)
$\dot{E}$	energy flow rate ( $\text{Kg}\cdot\text{m}/\text{s}^3$ )
$e_v$	friction loss factor
$f$	friction factor
$f_f$	volume fraction of liquid in tank
$g$	gravitational acceleration ( $\text{m}/\text{s}^2$ )
$h$	head loss in pipes (m)
$K$	energy loss coefficient
$K_{rt}$	energy loss coefficient for reversal losses at the draft tube bottom
$K_{ru}$	energy loss coefficient for reversal losses at the draft tube top
$K_L$	mass transfer coefficient
$L$	length (m)
$L_a$	depth of slurry (m)
$L_d$	length of draft tube (m)
$\dot{m}$	mass flow rate ( $\text{Kg}/\text{s}$ )
$P$	pressure ( $\text{N}/\text{m}^2$ )
$P_1$	atmospheric pressure
$P_2$	pressure at a point just above the gas distributor( $\text{N}/\text{m}^2$ )

$P_{ru}$	reversal losses at the draft tube top ( $N/m^3$ )
$\dot{Q}$	slurry flow rate in tank ( $m^3/s$ )
R	universal gas constant ( $Kg \cdot m^2/s^2 \cdot K$ )
$R_h$	hydraulic radius (m)
T	temperature (K)
$U_g$	superficial gas velocity based on cross sectional area of tank (m/s)
$U_{gc}$	critical superficial gas velocity based on cross sectional area of tank (m/s)
$U^*$	bulk slurry velocity in annulus (m/s)
V	velocity of slurry (m/s)
$\langle V \rangle$	average velocity of slurry (m/s)
$V_o, V_t$	terminal velocity of particles in stagnant liquid (m/s)
$V_a$	velocity of slurry in annulus (m/s)
$V_b$	velocity of slurry at the draft tube bottom (m/s)
$V_d$	velocity of slurry in draft tube (m/s)

#### Greek Symbols

$\rho$	density of water ( $Kg/m^3$ )
$\rho_m$	overall density of slurry ( $Kg/m^3$ )
$\rho_p$	density of particles ( $Kg/m^3$ )
$\phi$	volume fraction of solids in tank
$\phi_d$	volume fraction of gas phase in draft tube
$\mu$	viscosity of water ( $Kg/m \cdot s$ )
$\mu_m$	overall viscosity of slurry ( $Kg/m \cdot s$ )
$\nu$	kinematic viscosity ( $m^2/s$ )

#### Subscripts

a	annulus
d	draft tube
f	liquid

g	gas
m	slurry
p	particles
t	tank
1	top level of slurry in tank
2	at the level of gas distributor

## .1 Tables

Table-1

S. No.	Superficial Gas Velocity (m/s)	Volume Fraction	Drag Coefficient	Particle's Reynolds Number	Reynolds Number
1	$.6990 \times 10^{-2}$	$.2000 \times 10^{-1}$	.9656	116.0	48040
2	$.8587 \times 10^{-2}$	$.3000 \times 10^{-1}$	.9331	124.0	51330
3	$.9943 \times 10^{-2}$	$.4000 \times 10^{-1}$	.9108	129.9	53800
4	$.1115 \times 10^{-1}$	$.5000 \times 10^{-1}$	.8938	134.7	55800
5	$.1224 \times 10^{-1}$	$.6000 \times 10^{-1}$	.8803	138.8	57490
6	$.1326 \times 10^{-1}$	$.7000 \times 10^{-1}$	.8690	142.3	58950
7	$.1421 \times 10^{-1}$	$.8000 \times 10^{-1}$	.8594	145.5	60250
8	$.1597 \times 10^{-1}$	.1000	.8435	150.9	62480
9	$.1758 \times 10^{-1}$	.1200	.8308	155.4	64370
10	$.1908 \times 10^{-1}$	.1400	.8022	159.4	66010

Table-2a

Volume Fraction of Solids = .04

S. No.	Superficial Gas Velocity (m/s)	Particle Diameter	Terminal Velocity	Drag Coefficient	Particle's Reynolds Number	Reynolds Number
1	$.2265 \times 10^{-2}$	$.1170 \times 10^{-3}$	$.3845 \times 10^{-1}$	1.561	47.37	33197.7
2	$.3509 \times 10^{-2}$	$.1360 \times 10^{-3}$	$.4496 \times 10^{-1}$	1.327	63.60	38350.0
3	$.6135 \times 10^{-2}$	$.1660 \times 10^{-3}$	$.5499 \times 10^{-1}$	1.082	93.20	46036.3
4	$.9943 \times 10^{-2}$	$.1980 \times 10^{-3}$	$.6547 \times 10^{-1}$	.9108	129.9	53803.8
5	$.2050 \times 10^{-1}$	$.2580 \times 10^{-3}$	$.8475 \times 10^{-1}$	.7083	212.7	67596.7
6	$.3068 \times 10^{-1}$	$.2980 \times 10^{-3}$	$.9743 \times 10^{-1}$	.6190	277.8	76428.1
7	$.5251 \times 10^{-1}$	$.3580 \times 10^{-3}$	.1163	.5215	390.0	89334.6
8	$.7326 \times 10^{-1}$	$.3980 \times 10^{-3}$	.1289	.4722	474.6	97784.7
9	.1199	$.4580 \times 10^{-3}$	.1478	.4135	616.1	110311.1
10	.1707	$.4980 \times 10^{-3}$	.1604	.3818	720.3	118595.9



Table-2b

Volume Fraction of Solids = .08

S. No.	Superficial Gas Velocity (m/s)	Particle Diameter	Terminal Velocity	Drag Coeffi- cient	Particle's Reynolds Number	Reynolds Num- ber
1	$.3261 \times 10^{-2}$	$.1170 \times 10^{-3}$	$.3974 \times 10^{-1}$	1.461	53.37	37403.1
2	$.5025 \times 10^{-2}$	$.1360 \times 10^{-3}$	$.4639 \times 10^{-1}$	1.246	71.49	43102.0
3	$.8759 \times 10^{-2}$	$.1660 \times 10^{-3}$	$.5666 \times 10^{-1}$	1.019	104.5	51620.4
4	$.1421 \times 10^{-1}$	$.1980 \times 10^{-3}$	$.6740 \times 10^{-1}$	.8594	145.5	60248.7
5	$.2962 \times 10^{-1}$	$.2580 \times 10^{-3}$	$.8718 \times 10^{-1}$	.6693	237.9	75615.0
6	$.4489 \times 10^{-1}$	$.2980 \times 10^{-3}$	.1002	.5850	310.6	85480.0
7	$.7930 \times 10^{-1}$	$.3580 \times 10^{-3}$	.1197	.4927	436.3	99928.8
8	.1147	$.3980 \times 10^{-3}$	.1326	.4460	531.0	109406.5
9	.2118	$.4580 \times 10^{-3}$	.1521	.3904	689.7	123479.1
10	.3393	$.4980 \times 10^{-3}$	.1651	.3603	806.5	132800.1

Table-3a

Volume Fraction of Solids = .03

S. No.	Superficial Gas Velocity (m/s)	Draft Tube Length (m)	Drag Coeffi- cient	Particle's Reynolds Number	Reynolds Number
1	$.1408 \times 10^{-1}$	.50	.8561	146.6	60700
2	$.1086 \times 10^{-1}$	.85	.8948	134.4	55680
3	$.1005 \times 10^{-1}$	1.0	.9071	130.9	54230
4	$.9223 \times 10^{-2}$	1.2	.9211	127.1	52640
5	$.8587 \times 10^{-2}$	1.4	.9331	124.0	51330
6	$.1025 \times 10^{-1}$	1.6	.9071	130.9	54230
7	$.1031 \times 10^{-1}$	1.8	.9071	130.9	54230
8	$.1037 \times 10^{-1}$	2.0	.9071	130.9	54230
9	$.1041 \times 10^{-1}$	2.1	.9071	130.9	54230
10	$.1044 \times 10^{-1}$	2.2	.9071	130.9	54230

Table-3b

Volume Fraction of Solids = .08

S. No.	Superficial Gas Velocity (m/s)	Draft Tube Length (m)	Drag Coeffi- cient	Particle's Reynolds Number	Reynolds Number
1	$.2351 \times 10^{-1}$	.50	.7892	171.9	71190
2	$.1805 \times 10^{-1}$	.85	.8245	157.7	65330
3	$.1668 \times 10^{-1}$	1.0	.8357	153.6	63630
4	$.1528 \times 10^{-1}$	1.2	.8484	149.2	61780
5	$.1421 \times 10^{-1}$	1.4	.8594	145.5	60250
6	$.1699 \times 10^{-1}$	1.6	.8357	153.6	63630
7	$.1710 \times 10^{-1}$	1.8	.8357	153.6	63630
8	$.1721 \times 10^{-1}$	2.0	.8357	153.6	63630
9	$.1726 \times 10^{-1}$	2.1	.8357	153.6	63630
10	$.1731 \times 10^{-1}$	2.2	.8357	153.6	63630

Table-4a

Volume Fraction of Solids = .03

S. No.	Superficial Gas Velocity (m/s)	Draft Tube Diameter (m)	Ratio ( $D_d/D_t$ )	Drag Coeffi- cient	Particle's Reynolds Number	Reynolds Number
1	$.3183 \times 10^{-1}$	$.6200 \times 10^{-1}$	.4429	.8325	154.8	48474.5
2	$.2608 \times 10^{-1}$	$.6700 \times 10^{-1}$	.4786	.8140	161.8	54739.3
3	$.2088 \times 10^{-1}$	$.7200 \times 10^{-1}$	.5143	.7972	168.5	61272.8
4	$.1627 \times 10^{-1}$	$.7700 \times 10^{-1}$	.5500	.7820	175.0	68066.7
5	$.1234 \times 10^{-1}$	$.8200 \times 10^{-1}$	.5857	.7679	181.4	75113.2
6	$.9168 \times 10^{-2}$	$.8700 \times 10^{-1}$	.6214	.7550	187.5	82405.5
7	$.6901 \times 10^{-2}$	$.9200 \times 10^{-1}$	.6571	.7430	193.6	89937.3
8	$.5734 \times 10^{-2}$	$.9700 \times 10^{-1}$	.6929	.7318	199.4	97702.7
9	$.9459 \times 10^{-2}$	.1020	.7286	.7214	205.2	105696.4
10	$.2477 \times 10^{-1}$	.1070	.7613	.7115	210.8	113913.4

Table-4b

Volume Fraction of Solids = .08

S. No.	Superficial Gas Velocity (m/s)	Draft Tube Diameter (m)	Ratio ( $D_d/D_t$ )	Drag Coeffi- cient	Particle's Reynolds Number	Reynolds Number
1	$.3562 \times 10^{-1}$	$.6200 \times 10^{-1}$	.4429	.8188	159.9	50066.4
2	$.2912 \times 10^{-1}$	$.6700 \times 10^{-1}$	.4786	.8007	167.1	56535.1
3	$.2326 \times 10^{-1}$	$.7200 \times 10^{-1}$	.5143	.7843	174.0	63281.3
4	$.1809 \times 10^{-1}$	$.7700 \times 10^{-1}$	.5500	.7692	180.8	70296.2
5	$.1369 \times 10^{-1}$	$.8200 \times 10^{-1}$	.5857	.7555	187.3	77572.0
6	$.1015 \times 10^{-1}$	$.8700 \times 10^{-1}$	.6214	.7428	193.7	85101.6
7	$.7615 \times 10^{-2}$	$.9200 \times 10^{-1}$	.6571	.7310	199.9	92878.3
8	$.6307 \times 10^{-2}$	$.9700 \times 10^{-1}$	.6929	.7200	206.0	100896.3
9	$.1041 \times 10^{-1}$	.1020	.7286	.7097	211.9	109150.0
10	$.2739 \times 10^{-1}$	.1070	.7643	.7001	217.7	117634.3

# Bibliography

- [1] Akita, K. and F. Yoshida, 'Gas Holdup and Volumetric Mass Transfer Coefficient in Bubble Columns,' *Ind. Eng. Chem. Proc. Des. Dev.*, 12, 1973, p.76.
- [2] Akita, K. and F. Yoshida, 'Bubble Size, Interfacial Area and Liquid Phase Mass Transfer Coefficients in Bubble Columns,' *Ind. Eng. Chem. Proc. Des. Dev.*, 13, 1974, p.84.
- [3] Bach, H.F. and T.F. Pilhofer, 'Variation of Gas Holdup in Bubble Columns with Physical Properties of Liquid and Operating Parameters of Columns,' *Ger. Chem. Eng.*, 1, 1978, p.270.
- [4] Beard and Pruppacher.
- [5] Begovich, J.M. and J.S. Watson, 'Hydrodynamic Characteristics of Three Phase Fluidised Bed,' *Fluidization. Proc. 2<sup>nd</sup> Eng. Found. Conf.. ed., J.F. Davidson and D.C. Keairns* 1978, p.190.
- [6] Bhavraju, S.M., T.W.F. Russel, and H.W. Blanch, 'The Design of Gas Sparged Devices for Viscous Liquid Systems,' *AIChE Journal*, 24, 1978, p.454.
- [7] Botton, R., D. Cosserat and J.C. Carpenter, 'Influence of Column Diameter and High Gas Throughputs on The Operation of Bubble Column,' *Chem. Eng. J.*, 16, 1978, p.107.

- [8] Calderbank, P.H., 'Gas Absorption from Bubbles,' *The Chem. Engrs.*, 45, 1967, CE209.
- [9] Darton, R.C. and D. Harrison, 'Bubble Wake Structure in Three Phase Fluidization,' *Paper Presented At The International Fluid Conf., Asilomer, U.S.A.*, June, 1975a.
- [10] Darton, R.C. and D. Harrison, 'Gas and Liquid Holdup in Three Phase Fluidization,' *Chem. Eng. Sci.*, 30, 1975b, p.581.
- [11] Deckwer, W.D., I. Alder and A. Zaidi, 'A Comprehensive Study on  $CO_2$ -Interphase Mass Transfer in Vertical Cocurrent and Countercurrent Gas Flow,' *Can. J. Chem. Eng.*, 56, 1978, p.43.
- [12] Durand, E. and E. Condolios, 'Proceedings of Colloquium on Hydraulic Transport of Coal,' *Paper No. IV*, p.39.
- [13] Freedman, W. and J.F. Davidson, 'Holdup and Liquid Circulation in Bubble Columns,' *Trans. Inst. Chem. Engrs.*, 47, 1969, p.T251.
- [14] Govindrao, V.M.H., 'On The Dynamics of Bubble Column Slurry Reactors,' *Chem. Eng. J.*, 9, 1975, p.229.
- [15] Guth, E., and R. Simha, *em Kolloid-Z.*, 74, 1936, 266.
- [16] Hikita, H., et al., 'Gas Holdup in Bubble Column,' *Chem. Eng. J.*, 20, 1980, p.59.
- [17] Hills, J.H., 'The Operation of a Bubble Column at High Throughputs I. Gas Holdup Measurements,' *Chem. Eng. J.*, 12, 1976, p.89.
- [18] Hughmark, G.A., 'Holdup and Mass Transfer in Bubble Columns,' *Ind. Eng. Chem. Proc. Des. Dev.*, 6, 1967, p.218.

- [19] Imafuku, K., Y.T. Wang, K. Koide. and H. Kubota, 'The Behaviour of Suspended Solid Particles in The Bubble Column,' *J. of Chem. Japan*, 1(2), 1968, p.153.
- [20] Javdani, K., S. Schwalbe and J. Fischer, 'Multiphase Flow of Gas-Liquid and Gas-Coal Slurry Mixtures in Vertical Tubes,' *Argonne National Laboratory Report*, ANL-76,IL(1977),p.116.
- [21] Jeffrey, D.J., and A. Acrivos, 'The Rheological Properties of Suspension of Rigid Particles,' *AIChE Journal*, 22(3), 1976, p.417.
- [22] Kara, S., B.G. Kelkar and Y.T. Shah, 'Hydrodynamics and Axial Mixing in Three Phase Bubble Column,' *Ind. Eng. Chem. Proc. Des. Dev.*, 1981.
- [23] Kato, H. et al., 'A Study of an Airlift Pump for Solid Particles,' *Bull. JSME*, 18(117), 1975, p.286.
- [24] Kato, Y., et al., 'The Behaviour of Suspended Solid Particles and Liquid in Bubble Column,' *J. Chem. Eng. Japan*, 5, 1972, p.112.
- [25] Kato, Y., et al., 'The Behaviour of Suspended Solid Particles and Liquid in Bubble Column,' *Int. Chem. Eng.*, 12, 1972, p.182.
- [26] Koide, J., et al., 'Behaviour of Bubbles in Large Scale Bubble Columns,' *J. Chem. Eng. Japan*, 12, 1979, p.98.
- [27] Koide, K., et al., 'Critical Gas Velocity Required for Complete Suspension of Particles in Solid Suspended Bubble Columns with Draught Tube,' *J. Chem. Eng. Japan*, 17(4), 1984. p.368.
- [28] Kumar, A., et al., 'Bubble Swarm Characteristics in Bubble Columns,' *Can. J. Chem. Eng.*, 54, 1976, p.503.



- [29] Mersmann, A., 'Design and Scale-up of Bubble and Slurry Columns,, *Ger. Chem. Eng.*, 1, 1978, p.1.
- [30] Miyahar, T., M. Hamaguchi, Y. Sakeda and T. Takahashi, 'Size of Bubbles and Liquid Circulation in a Bubble Column with a Draft Tube and Sieve Plates.' *Can. J. of Chem. Eng.*, 6, 1986, p.718.
- [31] Narayanan, S. et al., 'Suspension of Solids by Mechanical Agitation,' *Chem. Eng. Sci.*, 24, 1969, p.223.
- [32] Pruppacher and Steinberger.
- [33] Rose, H.E. and R.A. Duckworth, *The Engineer*, 227(5903), 392(1969); 227(5904), 430(1969); 227(5905) , 478(1969).
- [34] Roco, M.C. and C.A. Shook, 'Critical Deposit Velocity in Slurry Flow.' *AIChE Journal*, 31(8), 1985, p.1401.
- [35] Roco, M.C. and C.A. Shook, 'Modeling of Slurry Flow: The Effect of Particle Size,' *Can. J. Chem. Eng.*, 61(8), 1983, p.494.
- [36] Schugerl, K., J. Lucke and U. Oels, 'Bubble Column Bioreactors,' *Adv. Biochem. Eng., ed., T.K. Ghose, A. Fiechter, and N. Blakeborog.* 7, 1977, p.1.
- [37] Shah, Y.T., et al., 'Design Parameters Estimation for Bubble Column Reactors.' *AIChE Journal*, 28(3), 1982, p.353.
- [38] Shekhar, R., and J.W. Evans, 'Fluid Flow in Pachuca (Air Agitated) Tanks: Part II. Mathematical Modeling of Flow in Pachuca Tanks.' *Metal Trans. B.* 1990. p.191

- [39] Ueyama, K. and T. Miyauchi, 'Properties of Recirculating Turbulent Two Phase Flow in Gas Bubble Columns,' *Ind. Eng. Chem. Process Des. Dev.*, 14, 1980, p.492.
- [40] Vasalos, I.A. et al., 'Experimental Techniques for Studying Fluid Dynamics of H-Coal Reactor,' *Coal Processing Tech., CEP Technical Manual*, 6, 1980, p.226.
- [41] Weiland, P., 'Influence of Draft Tube Diameter on Operation Behaviour of Airlift Loop Reactors,' *Ger. Chem. Eng.*, 7, 1984, p.374.
- [42] Ying, D.H., E.N. Givens and R.F. Weimer, 'Gas Holdup in Gas-liquid and Gas-liquid-Solid Flow Reactors,' *Ind. Eng. Chem. Process Des. Dev.*, 19, 1980, p.635.
- [43] Zundelovich, Y. and E. Vigdorchik, 'Calculation of The Minimal Impeller Rotation Speed and Power Input for Suspension of Solids ,' *Theory and Practice of Stirring in Liquid Media, Giprotnickel Design and Research Institute, Moscow*, 1973, p.257.
- [44] Zwietering, N., 'Suspending of Solid Particles in Liquid by Agitators,' *Chem. Eng. Sci.*, 8, 1958, p.244.
- [45] Brodkey R.S., 'The Phenomena of Fluid Motions,' *Addison-Wesley Publishing Co., New York*, 1967.
- [46] Govier, G.W. and K. Aziz, 'The Flow of Complex Mixtures in Pipes,' *Reinhold Publishing Corp., New York*, 1972.
- [47] Soo, S.L., 'Fluid Dynamics of Multiphase Systems,' *Blaisdell Publishing Co., New York*, 1967.
- [48] Streeter, V.L., 'Handbook of Fluid Dynamics,' *McGraw-Hill Book Co., New York*, 1961.

- [49] Wallis, G.B., 'One Dimensional Two Phase Flow,' *McGraw-Hill Book Co., New York*, 1969.
- [50] Zenz, F.A. and D.F. Othmer, 'Fluidization and Fluid Particle Systems,' *Reinhold Publishing Corp., New York*, 1960.

A 1148.50

7

673-072

A114836

Si64m

## Date Slip

This book is to be returned on the  
date last stamped.

This image shows a single sheet of white paper with horizontal blue or grey ruling lines. A solid vertical line runs down the center of the page, creating two equal-width columns. The top edge of the paper has a small tab-like cutout. The bottom edge features a series of small, evenly spaced holes, suggesting it was part of a binder or folder. The paper appears slightly aged or off-white.

ME - 1992 M. S/N. MAT

Th

673.072

Si 64 m

A114836